Nonlinear Dyn (2018) 94:2727–2747
https://doi.org/10.1007/s11071-018-4521-6

ORIGINAL PAPER

# Continuous sliding mode controllers for multi-input multi-output systems

**Hancheol Cho · Thanapat Wanichanon · Firdaus E. Udwadia**

Received: 5 September 2016 / Accepted: 13 August 2018 / Published online: 29 August 2018


**Abstract** This paper develops new continuous sliding mode controllers for multi-input multi-output mechanical systems in the presence of unknown, but bounded uncertainties in the given forces and in the masses. Assuming the absence of the uncertainties, a reference control input is first calculated using the fundamental equation of constrained motion that causes the system trajectories to exactly track the reference while minimizing a weighted $L^2$ norm of the control effort. Next, in the presence of realistic uncertainties in the given forces and in the masses, two continuous sliding mode controllers are derived according to whether the mass matrix is diagonal or not. In the diagonal case, each element of the control vector is independently designed, while in the nondiagonal case the control vector is handled as a whole because its elements are coupled to one another. The two controllers are continuous because no signum functions are used. It is also shown that various forms of control input are possible depending on the control requirements among which a simple proportional-integral-derivative-type controller is exemplified in this paper. Two numerical examples serve to demonstrate the accuracy and robustness of the control methodology suggested herein.

**Keywords** Sliding mode control · Chattering alleviation · Fundamental equation of constrained motion · Multi-input multi-output systems

H. Cho (✉)
Water Power Technologies Program, Sandia National Laboratories, Albuquerque, NM 87123, USA
e-mail: hancho@sandia.gov

T. Wanichanon
Department of Mechanical Engineering, Mahidol University, 25/25, Phutthamonthon, Nakorn Pathom 73170, Thailand
e-mail: thanapat.wan@mahidol.edu

F. E. Udwadia
Departments of Aerospace and Mechanical Engineering, Civil Engineering, Mathematics, and Information and Operations Management, University of Southern California, Los Angeles, CA 90089-1453, USA
e-mail: feuusc@gmail.com

## 1 Introduction

The precision reference-tracking control problem in the presence of system uncertainties has historically attracted a number of researchers due to its great practical importance in real life. Over the past few decades, there have been successful attempts to develop high-performance linear or nonlinear controllers that track given reference trajectories with high accuracy. Among them, nonlinear adaptive control [1], model predictive control [2], backstepping control [3], and sliding mode control [4,5] are worthy of attention. Sliding mode control (SMC) is especially widely used to cope with such uncertainties due to its simplicity and robustness. However, the robustness and high accuracy of SMC are obtained at the expense of *chattering* which results in high-frequency oscillations. This chattering problem, which leads to high-speed switching about the so-called

sliding surface, is caused by the discontinuous signum function used in standard sliding mode control in order to force the system's trajectories to be attracted to the sliding surface.

The most common way for reducing chattering is to replace the discontinuous signum function by continuous saturation or sigmoidal ones that approximately mimic the signum function [6,7]. Li et al. [8] proposed a proportional, integral, derivative (PID) control of sliding surface function to remove chattering. The main drawback of this controller is that the existence of the PID control gains satisfying the reachability condition is not always guaranteed. Another popular method that circumvents chattering is to use higher-order SMCs [9,10]. The second-order SMC (SOSMC) or the super twisting algorithm [11] is widely adopted for its simplicity and reduced information demand. The main strategy of the SOSMC is to force a sliding variable and its time derivative to zero using a discontinuous control. The actual control that is used is then derived by integrating this discontinuous control signal, thereby producing continuous control.

Recently, Udwadia and Wanichanon [12] extended the standard SMC method by using a number of continuous functions instead of the signum function, thereby eliminating the chattering problem. Although their controller does not exactly place the system's trajectories onto the sliding surface, the errors can be made as (arbitrarily) small as desired and an estimate of the error bounds can be simply obtained. This approach is applied to satellite formation flying in [13], and in [14] a simpler continuous SMC is derived by Cho et al. More general forms of continuous functions than those used in [12,13] can be used and special attention is paid to a PID-form, showing that the standard PID controller can be successfully used to control uncertain nonlinear systems with uncertainties in the given forces without the occurrence of any chattering. However, [14] ignores the effects of uncertainties in the mass matrix of the mechanical system. Later on, the general use of a SMC with the PID-form has been reinstated in [15]. In that paper, both the effects of uncertainties in the mass matrix and in the given force vector of the mechanical system are considered. However, it is assumed in [15] that the uncertainty in the mass matrix is sufficiently small compared with the nominal mass matrix and the validity of the proposed control strategy is not guaranteed in the presence of large measurement errors in the masses of the system.

The current paper extends the results of [14] and [15] to a larger class of nonlinear uncertain multi-input multi-output (MIMO) systems. In addition, the proposed approach allows for various continuous functions in the control signal depending on practical control requirements, and good performance can still be achieved even with a poor estimate for the uncertainties in the mass matrix and/or in the given force vector. First, when trajectory requirements on a nonlinear nominal system are given assuming no uncertainties, the reference control input is analytically derived. The strategy is based on a new result, called the fundamental equation of constrained motion (FECM), proposed in the field of analytical dynamics [16–19]. The control requirements are recast as constraints on the mechanical system. With this methodology, the reference control forces can be expressed succinctly in closed form whether the constraints are holonomic and/or nonholonomic, while all the nonlinearities inherited from the original system are carried without any approximations and/or linearizations. Next, additional sliding mode controllers are designed to compensate for the uncertainties in the mechanical system's mass matrix as well as in the given force (and/or torque) vector that the system is subjected to [20]. In the current study, two different sliding mode controllers are developed according to whether the mass matrix is diagonal or not that use continuous functions to remove chattering. Recently, there has been a great interest in the new SMC design to be insensitive to so-called mismatched uncertainties [21–23] where uncertainties exist in different channels from the control input. However, it is assumed in this paper that every degree of freedom of the mechanical system is controlled, and therefore there are no mismatched uncertainties in the system.

This paper has two main objectives. First, new continuous sliding mode controllers are proposed to ensure arbitrarily small errors as desired for a class of nonlinear MIMO systems affected by the uncertainties both in the mass matrix and in the given force vector. Second, the proposed sliding mode controllers are composed of continuous functions, thereby effectively removing chattering, and hence are suitable for various practical applications.

This paper is organized as follows. Section 2 describes the first controller that provides reference control input for given reference trajectories for a nominal system where no uncertainties are considered. Such a nominal system may be thought of as being our best

description of a given physical system using the available information about it. In Sect. 3, new sliding mode controllers are developed and augmented for robustness in the presence of uncertainties in the masses and in the given forces in our nominal system. Effectiveness of the proposed controllers is demonstrated in Sect. 4 by simulating two examples, and conclusions are provided in Sect. 5.

## 2 Exact reference-tracking control for nonlinear nominal systems with no uncertainties

In this paper, two different controllers will be combined to track the desired reference trajectory in the presence of system uncertainties. In this section, the first controller will be developed to provide a reference control input for the nonlinear nominal system. This nominal system is our best mathematical model of the actual physical system, given the information available. Without any constraints, the equation of motion of a dynamical system is described by the Lagrange's equation:

$$\mathbf{M}(\boldsymbol{q}, t)\,\ddot{\boldsymbol{q}} = \boldsymbol{Q}(\boldsymbol{q}, \dot{\boldsymbol{q}}, t), \tag{1}$$

or

$$\boldsymbol{a}(t) := \ddot{\boldsymbol{q}}(t) = \mathbf{M}^{-1}(\boldsymbol{q}, t)\,\boldsymbol{Q}(\boldsymbol{q}, \dot{\boldsymbol{q}}, t), \tag{2}$$

where $t$ represents time, $\boldsymbol{q}(t) = \left[q_1(t)\ q_2(t) \cdots q_n(t)\right]^{\mathrm{T}}$ is a generalized displacement vector, $\mathbf{M} > \mathbf{0}$ is an $n$ by $n$ mass matrix, $\boldsymbol{Q}$ is the $n$ by 1 'given' generalized force vector, and $\boldsymbol{a}(t)$ is the $n$ by 1 unconstrained acceleration vector. The superscript "$T$" denotes the transpose of a vector or a matrix, and $n$ is the number of the generalized coordinates.

Now, it is assumed that the unconstrained system described by Eq. (1) or (2) is subjected to $p$ constraints which are of the form

$$\varphi_j(\boldsymbol{q}, \dot{\boldsymbol{q}}, t) = 0, \quad j = 1, 2, \ldots, p. \tag{3}$$

These constraints can be thought of as control requirements imposed on the dynamical system and will be referred to later on in this paper as control constraints. Equation (3) includes all the usual varieties of holonomic and/or nonholonomic constraints and then some. Differentiating Eq. (3) with respect to time once (for nonholonomic constraints) or twice (for holonomic constraints) yields the following constraint equation:

$$\mathbf{A}\left[\boldsymbol{q}(t), \dot{\boldsymbol{q}}(t), t\right]\ddot{\boldsymbol{q}} = \boldsymbol{b}\left[\boldsymbol{q}(t), \dot{\boldsymbol{q}}(t), t\right], \tag{4}$$

where $\mathbf{A}$ is a $p$ by $n$ matrix and $\boldsymbol{b}$ is a $p$ by 1 vector. From here on for brevity, the arguments of the various quantities will be suppressed unless required for clarity.

Then, the aim is to obtain a vector $\ddot{\boldsymbol{q}}$ in closed form that satisfies the constraint equation, Eq. (4), and that simultaneously minimizes an additional control cost. First, the solution to Eq. (4) is explicitly given by [24, 25]:

$$\ddot{\boldsymbol{q}} = \mathbf{A}^{+}\boldsymbol{b} + \left(\mathbf{I} - \mathbf{A}^{+}\mathbf{A}\right)\boldsymbol{h}, \tag{5}$$

where $\mathbf{I}$ is the $n$ by $n$ identity matrix, the superscript "+" denotes the Moore–Penrose generalized inverse, and $\boldsymbol{h}$ is an arbitrary $n$ by 1 vector. From the perspective of controller design, it is generally desired to obtain this arbitrary $\boldsymbol{h}$ so that it minimizes the following cost function *at each instant of time*:

$$J = (\ddot{\boldsymbol{q}} - \boldsymbol{a})^{\mathrm{T}}\,\mathbf{M}\,(\ddot{\boldsymbol{q}} - \boldsymbol{a}). \tag{6}$$

Substituting $\boldsymbol{h}$ that minimizes Eq. (6) back to Eq. (5), one can finally obtain the following equation of motion in the presence of the constraints as [25]

$$\begin{aligned}\ddot{\boldsymbol{q}}(t) &= \boldsymbol{a}(t) + \mathbf{M}^{-1}\mathbf{A}^{\mathrm{T}}\left(\mathbf{A}\mathbf{M}^{-1}\mathbf{A}^{\mathrm{T}}\right)^{+}(\boldsymbol{b} - \mathbf{A}\boldsymbol{a}) \\ &=: \boldsymbol{a}(t) + \mathbf{M}^{-1}\boldsymbol{Q}^{c}(t),\end{aligned} \tag{7}$$

where the required (generalized) control force $\boldsymbol{Q}^{c}(t)$ is obtained in closed form:

$$\boldsymbol{Q}^{c}(t) := \mathbf{M}(\ddot{\boldsymbol{q}} - \boldsymbol{a}) = \mathbf{A}^{\mathrm{T}}\left(\mathbf{A}\mathbf{M}^{-1}\mathbf{A}^{\mathrm{T}}\right)^{+}(\boldsymbol{b} - \mathbf{A}\boldsymbol{a}). \tag{8}$$

This control force minimizes the quadratic control cost $J(t) = \left[\boldsymbol{Q}^{c}\right]^{\mathrm{T}}\mathbf{M}^{-1}\boldsymbol{Q}^{c}$ or Eq. (6) at each instant of time. (When using weighting matrices other than $\mathbf{M}^{-1}$ in the control cost, see [19]).

Originally, this idea is inspired by a recent finding in analytical dynamics [25,26] and Eq. (7) is called the fundamental equation of constrained motion (FECM). Equation (8) explicitly gives the control force, preserving all the nonlinearities of the original dynamical system. In what follows, the constraints given in Eq. (3) shall be interpreted as the trajectory requirements that the dynamical system described in Eq. (1) is required to track [18,19].

It is noted that the constraints, Eq. (3), have to be satisfied at each instant of time including the initial time ($t = 0$). However, it is generally difficult to meet these constraints from the beginning since this requires inserting the mass into the desired (constrained) manifold with the exact initial conditions. Hence, we need

to modify the constraint formulation in which new constraints are exactly satisfied over the whole time interval. First, let us write Eq. (3) in a compact form:

$$\boldsymbol{\varphi} = \left[\varphi_1\ \varphi_2\ \cdots\ \varphi_p\right]^{\mathrm{T}} = \mathbf{0}. \tag{9}$$

Now, it is assumed that Eq. (9) is not satisfied at the initial time such that $\boldsymbol{\varphi}(0) \neq \mathbf{0}$. Then, we modify the constraint equation, Eq. (9), to [18]

$$\ddot{\boldsymbol{\varphi}} + \boldsymbol{\alpha}\dot{\boldsymbol{\varphi}} + \boldsymbol{\beta}\boldsymbol{\varphi} = \mathbf{0},\ \boldsymbol{\alpha} = diag\left\{\alpha_1, \alpha_2, \ldots, \alpha_p\right\},\ \boldsymbol{\beta} = diag\left\{\beta_1, \beta_2, \ldots, \beta_p\right\}, \tag{10}$$

where $\boldsymbol{\varphi}$ comprises holonomic constraints. If $\boldsymbol{\varphi}$ is composed of nonholonomic constraints, then Eq. (9) is modified to

$$\dot{\boldsymbol{\varphi}} + \boldsymbol{\alpha}\boldsymbol{\varphi} = \mathbf{0},\ \boldsymbol{\alpha} = diag\left\{\alpha_1, \alpha_2, \ldots, \alpha_p\right\}. \tag{11}$$

By properly choosing the parameters $\alpha_i, \beta_i > 0$, $i = 1, 2, \ldots, p$, $\boldsymbol{\varphi}$ approaches zero asymptotically in a desired manner. More specifically, if Eq. (3) results in Eq. (4), then the modified constraint equations, Eqs. (10) and (11), respectively, yield

$$\mathbf{A}\ddot{\boldsymbol{q}} = \boldsymbol{b} - \boldsymbol{\alpha}\dot{\boldsymbol{\varphi}} - \boldsymbol{\beta}\boldsymbol{\varphi}, \tag{12a}$$

and

$$\mathbf{A}\ddot{\boldsymbol{q}} = \boldsymbol{b} - \boldsymbol{\alpha}\dot{\boldsymbol{\varphi}}, \tag{12b}$$

where the matrix $\mathbf{A}$ is unchanged and the vector $b$ is augmented by $-\boldsymbol{\alpha}\dot{\boldsymbol{\varphi}} - \boldsymbol{\beta}\boldsymbol{\varphi}$ or $-\boldsymbol{\alpha}\dot{\boldsymbol{\varphi}}$, which still retains the form of Eq. (4). In brief, using the new constraint equations, Eqs. (12a) and (12b), and the corresponding FECM, we can make the constraints satisfied at each instant of time during the control action including the initial time.

Up to now, the exact control force $\boldsymbol{Q}^c(t)$ has been developed assuming no uncertainties in the dynamical system. In the next section, a new additional controller will be derived and added in order to handle the effects of uncertainties.

## 3 New sliding mode control to cope with system uncertainties

A controller used in the real world is required to be robust in the sense that it can successfully track the reference trajectory regardless of uncertainty effects. Since MIMO systems are handled in this study, there must be interactions between the manipulated variables (inputs) and the controlled variables (outputs). These interactions can be quantified, for example, via the concept of the relative gain array (RGA) [27]. Roughly speaking, each element of the RGA is calculated as the ratio of the *open-loop* gain between the $i$th output and the $j$th input to the *closed-loop* gain between the $i$th ouput and the $j$th input. Refer to [27] for more details to compute the RGA. Plants with large RGA elements are in general difficult to control due to high sensitivity to uncertainties caused by strong interactions. However, it is assumed in this paper that the plant to be controlled does not have large RGA elements (at least at crossover frequency) so that uncertainty effects are successfully suppressed by the use of continuous sliding mode control techniques that will be developed in this section.

Sliding mode control is widely adopted to cope with uncertainties due to its simplicity and high robustness. However, one main drawback of the conventional sliding mode control is the chattering problem: high-frequency oscillations in the control forces and/or in the system's coordinates. In the present paper, hence, it will be shown that instead of the existing signum or saturation functions, many other continuous functions can be used to effectively avoid the chattering phenomenon, and one can have flexibility in prescribing values (or estimates) for the lower and/or upper uncertainty bounds.

For the constrained nominal system with no uncertainties, the equation of motion is given by

$$\mathbf{M}(\boldsymbol{q}, t)\,\ddot{\boldsymbol{q}} = \boldsymbol{Q}(\boldsymbol{q}, \dot{\boldsymbol{q}}, t) + \boldsymbol{Q}^c(t), \tag{13}$$

where $\mathbf{M}(\boldsymbol{q}, t)$ is the nominal mass matrix of the system, $\boldsymbol{Q}(\boldsymbol{q}, \dot{\boldsymbol{q}}, t)$ is the nominal 'given' (generalized) force vector, and $\boldsymbol{Q}^c(t)$ is the generalized control force that is explicitly given in Eq. (8) and is based on the description (and choice) of the nominal system. This generalized control force is added to exactly satisfy the given trajectory requirements (constraints) given in Eq. (3).

In the real world, however, it may often not be possible to exactly determine the *actual* mass matrix $\mathbf{M}_a(\boldsymbol{q}, t)$ and/or the *actual* 'given' force vector $\boldsymbol{Q}_a\left(\boldsymbol{q}, \dot{\boldsymbol{q}}, t\right)$ to which the actual system is subjected. Application of the control force $\boldsymbol{Q}^c(t)$ to the actual (unknown) system would result in the trajectory requirements (control constraints) given in Eq. (3) being, in general, not satisfied. Moreover, if $\boldsymbol{q}(t)$, $\dot{\boldsymbol{q}}(t)$, and $\ddot{\boldsymbol{q}}(t)$ obtained from the solution of Eq. (13) were substituted for $\hat{\boldsymbol{q}}(t)$, $\dot{\hat{\boldsymbol{q}}}(t)$, and $\ddot{\hat{\boldsymbol{q}}}(t)$ in the equation

$$\mathbf{M}_a\left(\hat{\boldsymbol{q}}, t\right)\ddot{\hat{\boldsymbol{q}}} \neq Q_a\left(\hat{\boldsymbol{q}}, \dot{\hat{\boldsymbol{q}}}, t\right) + \boldsymbol{Q}^c(t), \tag{14}$$

the left-hand side of this equation would, in general, not equal the right-hand side. In Eq. (14), $\mathbf{M}_a$ and $\boldsymbol{Q}_a$ are the actual (unknown) mass matrix and the actual (unknown) 'given' force vector, respectively. Thus, to successfully track the given reference trajectory (i.e., satisfy the trajectory requirements) in the presence of system uncertainties we add an additional controller $\boldsymbol{Q}^u(t)$ that compensates for the uncertainties, so that the equation of motion of the uncertain system becomes

$$\mathbf{M}_a\left(\boldsymbol{q}_c, t\right)\ddot{\boldsymbol{q}}_c = \boldsymbol{Q}_a\left(\boldsymbol{q}_c, \dot{\boldsymbol{q}}_c, t\right) + \boldsymbol{Q}^c(t) + \boldsymbol{Q}^u(t), \tag{15}$$

where $\boldsymbol{q}_c(t)$ and $\dot{\boldsymbol{q}}_c(t)$ denote the controlled, actual generalized displacement and velocity vectors, respectively. This additional (generalized) control force $\boldsymbol{Q}^u(t)$ will be developed by generalizing the concept of sliding mode control.

Pre-multiplying both sides of Eq. (15) by $\mathbf{M}_a^{-1}$, the acceleration of this controlled system can then be expressed as

$$\ddot{\boldsymbol{q}}_c = \boldsymbol{a}_a + \mathbf{M}_a^{-1}\boldsymbol{Q}^c(t) + \mathbf{M}_a^{-1}\mathbf{M}\boldsymbol{u}. \tag{16}$$

Here, $\boldsymbol{a}_a := \mathbf{M}_a^{-1}\boldsymbol{Q}_a$ and $\boldsymbol{Q}^u := \mathbf{M}\boldsymbol{u}$. $\mathbf{M}$ is the nominal mass matrix, and $u$ is the additional generalized acceleration vector provided by the additional control force $\boldsymbol{Q}^{\boldsymbol{u}}$ that compensates for uncertainties in our knowledge of the actual system.

*The aim is to control the actual (uncertain) system so that it tracks (mimics) the behavior of the nominal system, thereby making the actual system behave* ***as though*** *there was* ***no uncertainty*** *in the description of the* ***nominal system***.

Defining the tracking error as

$$\boldsymbol{e}(t) = \boldsymbol{q}_c(t) - \boldsymbol{q}(t) \tag{17}$$

[where $\boldsymbol{q}(t)$ is the response of the nominal system given by Eq. (13)], and differentiating Eq. (17) twice with respect to time, one has

$$\ddot{\boldsymbol{e}} = \ddot{\boldsymbol{q}}_c - \ddot{\boldsymbol{q}} \tag{18}$$

which upon use of Eqs. (7) and (16) yields

$$\begin{aligned}\ddot{\boldsymbol{e}} &= \left[\boldsymbol{a}_{\boldsymbol{a}}\left(\boldsymbol{q}_c, \dot{\boldsymbol{q}}_c, t\right) - a\left(\boldsymbol{q}, \dot{\boldsymbol{q}}, t\right)\right] \\ &\quad + \left[\mathbf{M}_a^{-1}\left(\boldsymbol{q}_c, t\right) - \mathbf{M}^{-1}\left(\boldsymbol{q}, t\right)\right]\boldsymbol{Q}^c(t) \\ &\quad + \mathbf{M}_a^{-1}\left(\boldsymbol{q}_c, t\right)\mathbf{M}\left(\boldsymbol{q}, t\right)\boldsymbol{u} \\ &=: \delta\ddot{\boldsymbol{q}} + \mathbf{M}_a^{-1}\mathbf{M}\boldsymbol{u},\end{aligned} \tag{19}$$

where the following has been defined:

$$\delta\ddot{\boldsymbol{q}}\left(\boldsymbol{q}, \dot{\boldsymbol{q}}, \boldsymbol{q}_c, \dot{\boldsymbol{q}}_c, t\right) := \left[\boldsymbol{a}_a\left(\boldsymbol{q}_c, \dot{\boldsymbol{q}}_c, t\right) - a\left(\boldsymbol{q}, \dot{\boldsymbol{q}}, t\right)\right]$$

$$+ \left[\mathbf{M}_a^{-1}\left(\boldsymbol{q}_c, t\right) - \mathbf{M}^{-1}\left(\boldsymbol{q}, t\right)\right]\boldsymbol{Q}^c(t). \tag{20}$$

Equation (19) points out that uncertainties in the actual system's description cause the dynamical mass matrix $\mathbf{M}_a\left(\boldsymbol{q}_c, t\right)$ and the (generalized) given force vector $\boldsymbol{Q}_a\left(\boldsymbol{q}_c, \dot{\boldsymbol{q}}_c, t\right)$ of the actual system to differ, in general, at each instant of time from those of the nominal system because of three reasons:

(1) the *parameters* (e.g., the masses, moments of inertia in the mass matrix, and the given forces in the generalized force vector) describing the actual system are different from those of the nominal system,
(2) the elements of the actual mass matrix and the actual given force vector may be different *functions* of their respective arguments from those of the corresponding elements of the nominal mass matrix and nominal 'given' force vector, and
(3) the controlled response of the actual system, $\boldsymbol{q}_c(t)$, is different from that of the nominal system, $\boldsymbol{q}(t)$. The former depends on the actual (generalized) forces acting on the system and the parameters that describe the actual system, both of which are only imprecisely known, as well as the additional control $\boldsymbol{Q}^u(t)$.

It should be noted that even if the parameters in the elements of the mass matrix are known with high precision along with their functional forms, uncertainties in the (generalized) given forces that act on the system will, in general, cause the mass matrix $\mathbf{M}_a$ of the actual system at any instant of time to differ from that of the nominal system $\mathbf{M}$ at that time, since $\mathbf{M}$ and $\mathbf{M}_a$ are in general functions of $\boldsymbol{q}(t)$ and $\boldsymbol{q}_c(t)$, respectively.

Since $\mathbf{M}_a$ and $\boldsymbol{Q}_a$ are uncertain, the value of $\delta\ddot{\boldsymbol{q}}$ at any instant of time is also uncertain. However, here it is assumed that one has a 'guestimate'—a guessed estimate based on experiments, experience, intuition, or otherwise—of a bound on it, so that

$$\|\delta\ddot{\boldsymbol{q}}\|_\infty < \Gamma, \tag{21}$$

where $\Gamma$ is a positive constant and $\|\cdot\|_\infty$ denotes the infinity norm of a vector or a matrix.

Now, let us consider the following two cases: 1) when the nominal mass matrix $\mathbf{M}$ and the actual mass matrix $\mathbf{M}_a$ are both diagonal and positive definite, and 2) when the nominal mass matrix $\mathbf{M}$ and the actual mass matrix $\mathbf{M}_a$ are both positive definite, but not necessarily diagonal.

### 3.1 Diagonal mass matrices

We assume that the $i$th diagonal elements of the matrices $\mathbf{M}_a$ and $\mathbf{M}$ are $\mu_i\left(\boldsymbol{q}_c, t\right) > 0$ and $m_i\left(\boldsymbol{q}, t\right) > 0$, respectively, for $i = 1, 2, \ldots, n$. Consider the generalized sliding surface $\boldsymbol{s}\left(t\right)$ given by

$$s\left(t\right) = \dot{e}\left(t\right) + \mathbf{B}\boldsymbol{e}\left(t\right) + \mathbf{K}\int \boldsymbol{e}\left(t\right) dt, \tag{22}$$

where $s\left(t\right) = \left[\begin{array}{cccc} s_1\left(t\right) & s_2\left(t\right) & \cdots & s_n\left(t\right)\end{array}\right]^{\mathrm{T}}$ and the $n$ by $n$ diagonal constant matrices $\mathbf{B}$ and $\mathbf{K}$ are given by

$$\mathbf{B} = \left[\begin{array}{cccc} b_1 & 0 & \cdots & 0 \\ 0 & b_2 & \cdots & 0 \\ \vdots & \vdots & \ddots & \vdots \\ 0 & 0 & \cdots & b_n \end{array}\right], \ \mathbf{K} = \left[\begin{array}{cccc} k_1 & 0 & \cdots & 0 \\ 0 & k_2 & \cdots & 0 \\ \vdots & \vdots & \ddots & \vdots \\ 0 & 0 & \cdots & k_n \end{array}\right], \tag{23}$$

with $b_i > 0$, $k_i \geq 0$ $(i = 1, 2, \ldots, n)$ so that $\mathbf{B}$ is positive definite and $\mathbf{K}$ is positive semi-definite. From Eq. (22), one has

$$s_i\left(t\right) = \dot{e}_i\left(t\right) + b_i e_i\left(t\right) + k_i \int e_i\left(t\right) dt, i = 1, 2, \ldots, n. \tag{24}$$

It is noted that if $s_i \equiv 0$, then $e_i$ converges to zero asymptotically as $t \to \infty$.

Now, let us define a Lyapunov function $V$ by:

$$V := \frac{1}{2}\boldsymbol{s}^{\mathrm{T}}\boldsymbol{s} = \frac{1}{2}\sum_{i=1}^{n} s_i^2. \tag{25}$$

Its time derivative is given by

$$\begin{aligned} \dot{V} = \boldsymbol{s}^{\mathrm{T}}\dot{\boldsymbol{s}} &= \sum_{i=1}^{n} s_i\dot{s}_i = \textstyle\sum_{i=1}^{n} s_i\left(\ddot{e}_i + b_i\dot{e}_i + k_i e_i\right) \\ &= \sum_{i=1}^{n} s_i\left(\delta\ddot{q}_i + \tfrac{m_i}{\mu_i}u_i + b_i\dot{e}_i + k_i e_i\right), \end{aligned} \tag{26}$$

where $u := \left[\begin{array}{ccc} u_1 & \cdots & u_n\end{array}\right]^{\mathrm{T}}$ and $\frac{m_i}{\mu_i}$ is the $i$th element of the $n$ by $n$ matrix $\mathbf{M}_a^{-1}\mathbf{M}$ which is diagonal, so that

$$\mathbf{M} = \left[\begin{array}{cccc} m_1 & 0 & \cdots & 0 \\ 0 & m_2 & \cdots & 0 \\ \vdots & \vdots & \ddots & \vdots \\ 0 & 0 & \cdots & m_n \end{array}\right], \ \mathbf{M}_a = \left[\begin{array}{cccc} \mu_1 & 0 & \cdots & 0 \\ 0 & \mu_2 & \cdots & 0 \\ \vdots & \vdots & \ddots & \vdots \\ 0 & 0 & \cdots & \mu_n \end{array}\right], \tag{27}$$

where $m_i\left(\boldsymbol{q}, t\right)$, are the known diagonal elements of the nominal mass matrix, whereas $\mu_i\left(\boldsymbol{q}_c, t\right)$ are the corresponding unknown elements of the actual mass matrix. We shall assume that the infinity norm of the inverse of the unknown actual mass matrix $\mathbf{M}_a^{-1}\left(\boldsymbol{q}_c, t\right)$ has lower and upper bounds so that

$$0 < \mu_m < \left\|\mathbf{M}_a^{-1}\right\|_{\infty} < \mu_M, \tag{28}$$

where $\mu_m$ and $\mu_M$ are positive constants, and it is assumed that one has their guestimates. Noting that $\mathbf{M}_a$ is diagonal, Eq. (28) can be rewritten as

$$\mu_m < \frac{1}{\mu_i\left(\boldsymbol{q}_c, t\right)} < \mu_M, i = 1, 2, \ldots, n. \tag{29}$$

Then, the aim is to find an additional control force $u_i$ so that $\dot{V}$ in Eq. (26) is negative. The conventional sliding mode controller utilizes the following control force $u_i$:

$$u_i = -\frac{1}{m_i}\left[\frac{b_i\dot{e}_i + k_i e_i}{\sqrt{\mu_m\mu_M}} + K_i\,\mathrm{sgn}\left(s_i\right)\right], \tag{30}$$

where $m_i$ is the $i$th element of the nominal mass matrix $\mathbf{M}$, and the gain $K_i$ is given by [28]:

$$K_i = \frac{\Gamma + \left(1 - \sqrt{\frac{\mu_m}{\mu_M}}\right)\left|b_i\dot{e}_i + k_i e_i\right|}{\mu_m}. \tag{31}$$

However, the discontinuity of the $\mathrm{sgn}\left(\cdot\right)$ function in Eq. (30) generally results in undesirable chattering. Instead, let us first consider a region where the condition $|s_i| > \varepsilon$ holds where $\varepsilon$ is a (small, user-prescribed) positive number. As shown in Appendix, the following inequality is then satisfied:

$$s_i\delta\ddot{q}_i < \frac{\Gamma}{\varepsilon}s_i^2. \tag{32}$$

Then, using relation (32), Eq. (26) becomes

$$\begin{aligned} \dot{V} &= \sum_{i=1}^{n} s_i\left(\delta\ddot{q}_i + \frac{m_i}{\mu_i}u_i + b_i\dot{e}_i + k_i e_i\right) \\ &< \sum_{i=1}^{n}\left[\frac{\Gamma}{\varepsilon}s_i^2 + s_i\left(\frac{m_i}{\mu_i}u_i + b_i\dot{e}_i + k_i e_i\right)\right]. \end{aligned} \tag{33}$$

Let us choose the additional acceleration $u_i$ according to the relation

$$u_i = -\frac{1}{m_i}\left[\frac{\Gamma}{\varepsilon\mu_m}s_i + \frac{1}{D_i}\left(b_i\dot{e}_i + k_i e_i\right) + f_i\left(s_i\right)\right], \tag{34}$$

where $f_i\left(s_i\right)$ is a function to be determined and the constant $D_i$ is chosen by the following rule:

$$D_i = \begin{cases} \mu_m, & \text{when } s_i\left(b_i\dot{e}_i + k_i e_i\right) \geq 0, \\ \mu_M, & \text{when } s_i\left(b_i\dot{e}_i + k_i e_i\right) < 0. \end{cases} \tag{35}$$

Then, Eq. (33) becomes

$$\begin{aligned} \dot{V} &< \sum_{i=1}^{n}\left[\frac{\Gamma}{\varepsilon}s_i^2 + s_i\left(\frac{m_i}{\mu_i}u_i + b_i\dot{e}_i + k_i e_i\right)\right] \\ &= \sum_{i=1}^{n}\left[\frac{\Gamma}{\varepsilon}\left(1 - \frac{1}{\mu_m\mu_i}\right)s_i^2\right. \\ &\quad \left. + s_i\left(b_i\dot{e}_i + k_i e_i\right)\left(1 - \frac{1}{D_i\mu_i}\right) - \frac{s_i}{\mu_i}f_i\left(s_i\right)\right]. \end{aligned} \tag{36}$$

It is noted that the first term $\frac{\Gamma}{\varepsilon}\left(1-\frac{1}{\mu_m\mu_i}\right)s_i^2$ and the second term $s_i\left(b_i\dot{e}_i+k_ie_i\right)\left(1-\frac{1}{D_i\mu_i}\right)$ in Eq. (36) are always negative. In brief, in the region $|s_i|>\varepsilon$, $\dot{V}<0$ is guaranteed by using Eq. (34) when $f_i\left(s_i\right)=0$ or, when $s_i$ and $f_i\left(s_i\right)$ have the same sign. Conventionally, the discontinuous signum function is used as noted in Eq. (30), resulting in the chattering problem, but now one can find a number of continuous functions $f_i\left(s_i\right)$ that do not suffer from such chattering. Though the discontinuity of $D_i$ in $u_i$ could cause chattering, the chattering effect can be effectively diminished by allowing the first term in Eq. (34) to dominate the second term; else, one can freely use a suitable function $f_i\left(s_i\right)$ (and/or gain) for the third term so that it dominates the second.

Selection of the function $f_i\left(s_i\right)$ will depend on, for example, the control performance associated with the control requirements. In this paper, special attention is paid to the case where

$$f_i\left(s_i\right)=\eta_i s_i,\quad\left(\eta_i\geq 0\right) \tag{37}$$

so that $s_i$ and $f_i\left(s_i\right)$ have the same sign and $\dot{V}<0$ is guaranteed. Then, using Eqs. (34) and (37) the control law $u_i\left(t\right)$ is given by

$$\begin{aligned}u_i\left(t\right)&=-\frac{1}{m_i}\left[\frac{\Gamma}{\varepsilon\mu_m}s_i+\frac{1}{D_i}\left(b_i\dot{e}_i+k_ie_i\right)+\eta_is_i\right]\\&=\frac{1}{m_i}\left[-\left(\frac{k_i}{D_i}+\frac{\Gamma b_i}{\varepsilon\mu_m}+\eta_ib_i\right)e_i\right.\\&\quad\left.-k_i\left(\frac{\Gamma}{\varepsilon\mu_m}+\eta_i\right)\int e_i\,dt-\left(\frac{b_i}{D_i}+\frac{\Gamma}{\varepsilon\mu_m}+\eta_i\right)\dot{e}_i\right]\\&=:\frac{1}{m_i}\left(G_{Pi}e_i+G_{Ii}\int e_i\,dt+G_{Di}\dot{e}_i\right),\end{aligned} \tag{38}$$

where $k_i\geq 0$, $b_i>0$, $\varepsilon>0$, $\Gamma>0$, and $\eta_i\geq 0$. Equation (38) shows that the control $u_i\left(t\right)$ is nothing but conventional PID control with the control gains given by

$$\begin{aligned}G_{Pi}&=-\left(\frac{k_i}{D_i}+\frac{\Gamma b_i}{\varepsilon\mu_m}+\eta_ib_i\right),\\G_{Ii}&=-k_i\left(\frac{\Gamma}{\varepsilon\mu_m}+\eta_i\right),\\G_{Di}&=-\left(\frac{b_i}{D_i}+\frac{\Gamma}{\varepsilon\mu_m}+\eta_i\right).\end{aligned} \tag{39}$$

Up to now, it has been shown that in the region $|s_i|>\varepsilon$, $\dot{V}<0$ is guaranteed if the control law, Eq. (34), is used where $f_i\left(s_i\right)=0$ or $s_i$ and $f_i\left(s_i\right)$ have the same sign. If, on the contrary, $|s_i|\leq\varepsilon$, $\dot{V}<0$ is not guaranteed and the errors may not converge to zero (although they are bounded). This is because the control $u_i\left(t\right)$ forces the states into the region bounded by $|s_i|\leq\varepsilon$ instead of onto the sliding surface $|s_i|=0$. However, $\varepsilon$ can be made as small as desired, so that the errors can accordingly be controlled to user-prescribed demands.

### 3.2 Positive definite mass matrices

If $\mathbf{M}$ and $\mathbf{M}_a$ are not diagonal, the procedure introduced in Sect. (3.1) does not apply because the elements in the additional control vector, $\boldsymbol{u}$, get coupled to one another. In this case, a different approach is used, which should encompass the previous case where the mass matrix is diagonal. However, unlike the previous case the matrix 2-norm will be used to prove Lyapunov stability.

When $\mathbf{M}$ and $\mathbf{M}_a$ are positive definite, we again define the Lyapunov function as Eq. (25) and its first derivative satisfies

$$\begin{aligned}\dot{V}&=\boldsymbol{s}^{\mathrm{T}}\dot{\boldsymbol{s}}=\boldsymbol{s}^{\mathrm{T}}\left[\delta\ddot{\boldsymbol{q}}+\mathbf{M}_a^{-1}\mathbf{M}\boldsymbol{u}+\left(\mathbf{B}\dot{\boldsymbol{e}}+\mathbf{K}\boldsymbol{e}\right)\right]\\&<\tfrac{\Gamma}{\varepsilon}\boldsymbol{s}^{\mathrm{T}}\boldsymbol{s}+\boldsymbol{s}^{\mathrm{T}}\left[\mathbf{M}_a^{-1}\mathbf{M}\boldsymbol{u}+\left(\mathbf{B}\dot{\boldsymbol{e}}+\mathbf{K}\boldsymbol{e}\right)\right],\end{aligned} \tag{40}$$

where $\mathbf{B}$ and $\mathbf{K}$ are defined in Eq. (23). The last inequality is proved in Appendix for the case $|s_i|>\varepsilon$. As in [29], we assume that the *2-norm* of the unknown actual mass matrix is bounded by

$$0<\|\mathbf{M}_a\|_2<\lambda_M, \tag{41}$$

where $\|\cdot\|_2$ denotes the 2-norm of a matrix and the lower bound of $\|\mathbf{M}_a\|_2$ need not be known. Since the matrix $\mathbf{M}_a$ is positive definite, Eq. (41) implies that the largest eigenvalue associated with $\mathbf{M}_a$ is bounded by a positive constant $\lambda_M$. Many analytical or numerical approaches [30,31] are known to estimate this upper bound. Next, we choose the additional control vector, $\boldsymbol{u}$, as

$$\boldsymbol{u}=-\mathbf{M}^{-1}\left(\frac{\lambda_M\Gamma}{\varepsilon}s+\frac{\lambda_M\left\|\mathbf{B}\dot{\boldsymbol{e}}+\mathbf{K}\boldsymbol{e}\right\|_\infty}{\varepsilon}\boldsymbol{s}+\boldsymbol{f}\left(s\right)\right). \tag{42}$$

Substituting Eq. (42) into Eq. (40) yields

$$\begin{aligned}\dot{V}<&\left(\frac{\Gamma}{\varepsilon}s^{\mathrm{T}}s-\frac{\lambda_M\Gamma}{\varepsilon}s^{\mathrm{T}}\mathbf{M}_a^{-1}s\right)\\&+\left(s^{\mathrm{T}}\left(\mathbf{B}\dot{\boldsymbol{e}}+\mathbf{K}\boldsymbol{e}\right)-\lambda_M\frac{\left\|\mathbf{B}\dot{\boldsymbol{e}}+\mathbf{K}\boldsymbol{e}\right\|_\infty}{\varepsilon}s^{\mathrm{T}}\mathbf{M}_a^{-1}s\right)\\&-\boldsymbol{s}^{\mathrm{T}}\mathbf{M}_a^{-1}\boldsymbol{f}\left(s\right).\end{aligned} \tag{43}$$

The first term, $\left(\frac{\Gamma}{\varepsilon}s^{\mathrm{T}}s-\frac{\lambda_M\Gamma}{\varepsilon}s^{\mathrm{T}}\mathbf{M}_a^{-1}\boldsymbol{s}\right)$, is less than zero because

$$\boldsymbol{s}^{\mathrm{T}}\mathbf{M}_a^{-1}\boldsymbol{s}>\frac{1}{\lambda_M}s^{\mathrm{T}}\boldsymbol{s}. \tag{44}$$

Similarly, the second term on the right in relation (43), when $|s_i| > \varepsilon$ holds, yields

$$\begin{aligned} & \boldsymbol{s}^{\mathrm{T}}\left(\mathbf{B}\dot{\boldsymbol{e}}+\mathbf{K}\boldsymbol{e}\right)-\frac{\lambda_M\left\|\mathbf{B}\dot{\boldsymbol{e}}+\mathbf{K}\boldsymbol{e}\right\|_\infty}{\varepsilon}\boldsymbol{s}^{\mathrm{T}}\mathbf{M}_a^{-1}\boldsymbol{s} \\ & \quad < \boldsymbol{s}^{\mathrm{T}}\left(\mathbf{B}\dot{\boldsymbol{e}}+\mathbf{K}\boldsymbol{e}\right)-\frac{\left\|\mathbf{B}\dot{\boldsymbol{e}}+\mathbf{K}\boldsymbol{e}\right\|_\infty}{\varepsilon}\boldsymbol{s}^{\mathrm{T}}\boldsymbol{s} \\ & \quad = \sum_{i=1}^{n}\left[s_i\left(b_i\dot{e}_i+k_ie_i\right)-\left\|\mathbf{B}\dot{\boldsymbol{e}}+\mathbf{K}\boldsymbol{e}\right\|_\infty\frac{s_i^2}{\varepsilon}\right]<0. \end{aligned} \tag{45}$$

In brief, the first and the second terms in Eq. (43) are less than zero, so if the third term, $-\boldsymbol{s}^{\mathrm{T}}\mathbf{M}_a^{-1}\boldsymbol{f}\left(\boldsymbol{s}\right)$, is zero or negative, $\dot{V} < 0$ is guaranteed. The selection of $\boldsymbol{f}\left(\boldsymbol{s}\right)$ will again depend on the control requirements, and let us consider the following case as in the previous subsection:

$$\boldsymbol{f}\left(s\right)=\eta\boldsymbol{s},\quad(\eta\geq 0) \tag{46}$$

where $\eta$ is a nonnegative constant. Then $-\boldsymbol{s}^{\mathrm{T}}\mathbf{M}_a^{-1}\boldsymbol{s}$ is negative, since $\mathbf{M}_a^{-1} > 0$. Now using Eqs. (42) and (46), the control law is explicitly given by

$$\begin{aligned} \boldsymbol{u} &= -\mathbf{M}^{-1}\left(\frac{\lambda_M\Gamma}{\varepsilon}\boldsymbol{s}+\lambda_M\frac{\left\|\mathbf{B}\dot{\boldsymbol{e}}+\mathbf{K}\boldsymbol{e}\right\|_\infty}{\varepsilon}\boldsymbol{s}+\eta\boldsymbol{s}\right) \\ &= -\mathbf{M}^{-1}\left(\frac{\lambda_M\Gamma}{\varepsilon}+\lambda_M\frac{\left\|\mathbf{B}\dot{\boldsymbol{e}}+\mathbf{K}\boldsymbol{e}\right\|_\infty}{\varepsilon}+\eta\right)\boldsymbol{s} \\ &= \mathbf{M}^{-1}\left[-\left(\frac{\lambda_M\Gamma}{\varepsilon}+\lambda_M\frac{\left\|\mathbf{B}\dot{\boldsymbol{e}}+\mathbf{K}\boldsymbol{e}\right\|_\infty}{\varepsilon}+\eta\right)\right. \\ &\quad \left.\times\left(\dot{\boldsymbol{e}}+\mathbf{B}\boldsymbol{e}+\mathbf{K}\int\boldsymbol{e}dt\right)\right] \\ &=: \mathbf{M}^{-1}\left(\mathbf{G}_P\boldsymbol{e}+\mathbf{G}_I\int\boldsymbol{e}dt+\mathbf{G}_D\dot{\boldsymbol{e}}\right). \end{aligned} \tag{47}$$

Equation (47) shows that the control $\boldsymbol{u}\left(t\right)$ is again a simple PID control with the control gains given by

$$\mathbf{G}_P=-\rho\mathbf{B},\ \mathbf{G}_I=-\rho\mathbf{K},\ \mathbf{G}_D=-\rho\mathbf{I}, \tag{48}$$

where $\rho := \frac{\lambda_M\Gamma}{\varepsilon}+\lambda_M\frac{\left\|\mathbf{B}\dot{\boldsymbol{e}}+\mathbf{K}\boldsymbol{e}\right\|_\infty}{\varepsilon}+\eta$.

As in the previous subsection, $\dot{V} < 0$ has been proved when $|s_i| > \varepsilon$. By choosing $\varepsilon$ small enough, one can achieve a user-prescribed level of the tracking error. Since the control is a continuous function, the chattering problem is circumvented.

In conclusion, two different additional controllers, $\boldsymbol{u}$, have been developed according to whether the mass matrices $\mathbf{M}$ and $\mathbf{M}_a$ are both diagonal and nondiagonal but positive definite. The first controller uses the infinity norm of the matrix, $\mathbf{M}_a^{-1}$, and only applies when the mass matrices are known to have a diagonal structure.

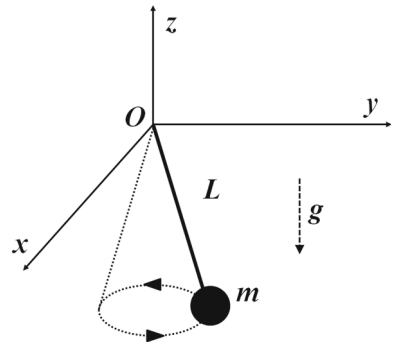


**Fig. 1** Spherical pendulum under air drag

Also, it may have a small amount of chattering because of the discontinuity of the gain $D_i$ given by Eq. (35), but the other high gains in the expression for $\boldsymbol{u}$ can be used to successfully mitigate this chattering effect. The second controller uses the 2-norm of the matrix $\mathbf{M}_a$ (i.e., the largest eigenvalue) and is more general in that it can be applied regardless of whether the mass matrix is diagonal or not. Also, chattering is completely eliminated because only continuous functions are used.

## 4 Numerical examples

In this section, two numerical examples are given to illustrate the control methodology developed in the previous sections.

### 4.1 Spherical pendulum

In the first example, we first consider a nominal system (with no uncertainty) which comprises a 3-dimensional pendulum that has a bob of mass $m$ that is suspended from a massless rod of length $L$. Besides the force of gravity, it is also affected by air drag (see Fig. 1). An inertial frame of reference is fixed at the point of suspension, $O$, of the pendulum, and the equation of motion of the pendulum without any constraint on its motion is given by

$$\begin{aligned} \boldsymbol{a}\left(t\right) &= \begin{bmatrix} a_x\left(t\right) \\ a_y\left(t\right) \\ a_z\left(t\right) \end{bmatrix} = \begin{bmatrix} 0 \\ 0 \\ -g \end{bmatrix} + \frac{gz-\dot{x}^2-\dot{y}^2-\dot{z}^2}{x^2+y^2+z^2} \\ &\quad \times \begin{bmatrix} x \\ y \\ z \end{bmatrix} - \frac{1}{2}C_D\frac{S_{\mathrm{ref}}}{m}\rho_0\left\|\boldsymbol{v}\right\|_2\begin{bmatrix} \dot{x} \\ \dot{y} \\ \dot{z} \end{bmatrix}, \end{aligned} \tag{49}$$

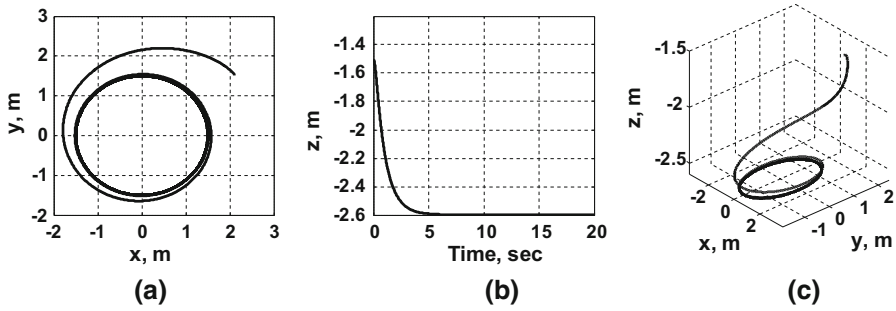


**Fig. 2** Nominal trajectories **a** in the $x-y$ plane, **b** along the $z$-axis, and **c** in 3 dimensions

where $g$ is the gravitational acceleration, $\left[x\ y\ z\right]^{\mathrm{T}}$ and $\left[\dot{x}\ \dot{y}\ \dot{z}\right]^{\mathrm{T}}$ are the position vector and the velocity vector of the mass in the inertial frame, respectively. Also, $C_D$ is the drag coefficient, $S_{\mathrm{ref}}$ is the cross-sectional area of the mass, and $\rho_0$ is the air density, all of which are assumed to be constant, and $\|\boldsymbol{v}\|_2 = \sqrt{\dot{x}^2+\dot{y}^2+\dot{z}^2}$ is the Euclidean norm of the velocity vector. In the numerical example, the nominal values $L = 3$ (m), $m = 5$ (kg), $g = 9$ (m/s$^2$), $C_D = 0.6$, $S_{\mathrm{ref}} = 0.01\pi$ (m$^2$), and $\rho_0 = 1.2754$ (kg/m$^3$) are assumed. It is noted that the mass matrix is given by

$$\mathbf{M}(\boldsymbol{q}, t) = m\mathbf{I}_{3\times 3}, \tag{50}$$

which is diagonal so the control law, Eq. (34), is applied in this first example.

Next, we describe two constraints (control requirements) on this pendulum so that

$$x^2+y^2 = \frac{L^2}{4}, \tag{51a}$$

$$z = -\frac{\sqrt{3}}{2}L, \tag{51b}$$

as shown in Fig. 1. It is noted that the initial conditions in the inertial frame used for the simulation do not satisfy the constraints, Eqs. (51a) and (51b), which are chosen as follows:

$$x_0 = \frac{L}{\sqrt{2}}\ (\mathrm{m}),\ \ y_0 = \frac{L}{2}\ (\mathrm{m}),\ z_0 = -\frac{L}{2}\ (\mathrm{m}),$$
$$\dot{x}_0 = -\sqrt{2}\ (\mathrm{m/s}),\ \dot{y}_0 = 2\ (\mathrm{m/s}),\ \dot{z}_0 = 0\ (\mathrm{m/s}). \tag{52}$$

Since Eqs. (51a) and (51b) are holonomic constraints, we employ Eq. (10) instead of Eq. (9). Differentiating Eqs. (51a) and (51b) with respect to time twice to get the form of Eq. (12a) yields

$$\begin{bmatrix} 2x & 2y & 0 \\ 0 & 0 & 1 \end{bmatrix}\begin{bmatrix} \ddot{x} \\ \ddot{y} \\ \ddot{z} \end{bmatrix} = \begin{bmatrix} -2\dot{x}^2-2\dot{y}^2-\alpha\left(2x\dot{x}+2y\dot{y}\right)-\beta\left(x^2+y^2-\frac{L^2}{4}\right) \\ -\alpha\dot{z}-\beta\left(z+\frac{\sqrt{3}}{2}L\right) \end{bmatrix} = \begin{bmatrix} b_1 \\ b_2 \end{bmatrix}, \tag{53}$$

where $\alpha = \alpha_1 = \alpha_2 = 6$ and $\beta = \beta_1 = \beta_2 = 5$ are assumed. The required nominal control force, $\boldsymbol{Q}^c(t)$, to exactly track this circular orbit is then given by the FECM as described in Eq. (8). Its form is explicitly given by

$$\boldsymbol{Q}^c(t) = m\begin{bmatrix} \frac{x}{2x^2+2y^2}\left(b_1-2xa_x-2ya_y\right) \\ \frac{y}{2x^2+2y^2}\left(b_1-2xa_x-2ya_y\right) \\ b_2-a_z \end{bmatrix}, \tag{54}$$

where $a_x$, $a_y$, $a_z$ are given in Eq. (49), and $b_1$, $b_2$ are found in Eq. (53).

Numerical integration in this example is carried out in the MATLAB/Simulink environment, using a fixed time step of 0.0001 second and the ode5 Dormand-Prince integrator. Figure 2 shows the nominal trajectories in the $x-y$ plane, along the $z$-axis, and in 3 dimensions. Figure 3 depicts the errors in the satisfaction of the two constraints, Eqs. (51a) and (51b), where we define the errors $e_1(t) := x^2+y^2-\frac{L^2}{4}$ and $e_2(t) := z+\frac{\sqrt{3}}{2}L$. Without assuming uncertainties, the control force $\boldsymbol{Q}^c(t)$ given by Eq. (54) makes the system trajectories asymptotically track the trajectory requirements given in Eqs. (51a) and (51b), despite the initial nonzero errors along each axis.

Now, it is assumed that the mass, the gravitational acceleration, and the drag coefficient are all only imprecisely known, and their actual values (unknown to us) are, respectively, $m_a = 6$ (kg), $g_a = 9.81$ (m/s$^2$), and $C_{D,a} = 0.47$. Then, the uncertainty caused by the imprecise information is given by

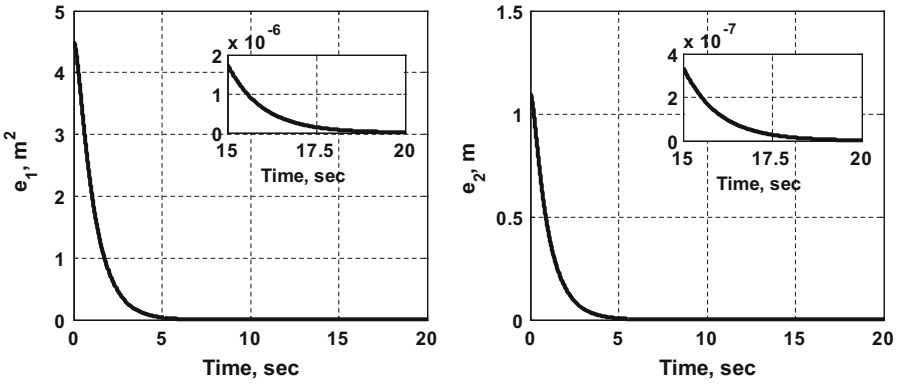


**Fig. 3** Errors in the satisfaction of Eqs. (51a) and (51b) when the control force Eq. (54) is applied for the nominal system

$$\delta\ddot{\boldsymbol{q}}(t) = [\boldsymbol{a}_a(t) - \boldsymbol{a}(t)] + \left(\mathbf{M}_a^{-1} - \mathbf{M}^{-1}\right)\boldsymbol{Q}^c(t), \tag{55}$$

where

$$\begin{aligned}\boldsymbol{a}_a(t) = &\begin{bmatrix}0\\0\\-g_a\end{bmatrix} + \frac{g_a z_c - \dot{x}_c^2 - \dot{y}_c^2 - \dot{z}_c^2}{x_c^2 + y_c^2 + z_c^2}\begin{bmatrix}x_c\\y_c\\z_c\end{bmatrix}\\ &-\tfrac{1}{2}C_{D,a}\tfrac{S_{\text{ref}}}{m_a}\rho_0\|v_c\|_2\begin{bmatrix}\dot{x}_c\\\dot{y}_c\\\dot{z}_c\end{bmatrix},\\ \mathbf{M}_a^{-1} = \tfrac{1}{m_a}\mathbf{I}_{3\times3},\ &\mathbf{M}^{-1} = \tfrac{1}{m}\mathbf{I}_{3\times3},\end{aligned} \tag{56}$$

and $\boldsymbol{a}(t)$ and $\boldsymbol{Q}^c(t)$ are given in Eqs. (49) and (54), respectively. Were this uncertainty to be completely ignored, and only the control, $\boldsymbol{Q}^c(t)$, that was obtained earlier using the FECM with the nominal system employed, the actual pendulum's trajectory would no longer be circular. Figure 4 shows the resulting errors in the trajectory of the actual pendulum in the satisfaction of the two constraints (Eqs. 51a and 51b). As seen in the figure, the two constraints (with the additional controller set to $\boldsymbol{u} = \mathbf{0}$) are not satisfied when the parameters describing the system and the forces acting on it are uncertain.

In order to compare the new continuous sliding mode controller developed in this paper with other robust control methods, the necessary control action taking into account the uncertainty is next obtained using the conventional PID controller which is of the form:

$$\boldsymbol{u} = K_P\boldsymbol{e} + K_I\int \boldsymbol{e}dt + K_D\dot{\boldsymbol{e}}, \tag{57}$$

where the PID gains are fine-tuned as $K_P = -1200$, $K_I = -3000$, and $K_D = -45$. Figures 5 and 6 plot the time histories of the tracking errors and the additional control forces, respectively. The tracking errors plotted in Fig. 5 represent the difference between the actual, controlled positions ($\boldsymbol{q}_c(t)$) and the nominal positions ($\boldsymbol{q}(t)$) shown in Fig. 2. The trajectories of the actual system controlled by the additional PID control action $\boldsymbol{u}$ follow closely those of the nominal system and hence have not been shown for brevity. The errors are relatively small, compared with Fig. 4, and it will be shortly shown that these errors can get smaller by employing the new continuous sliding mode controller proposed in this paper.

Next, the necessary control command in the presence of the uncertainties is obtained via the conventional sliding mode controller (Eq. 30). The parameters for the controller $\boldsymbol{u}$, are chosen as $b_i = 10$ and $k_i = 5$, and the lower and upper bounds for the mass uncertainty are set to $\mu_m = 0.1$ and $\mu_M = 0.3$. Also, the upper bound of the uncertainty $\|\delta\ddot{\boldsymbol{q}}\|_\infty$ is set to $\Gamma = 2$, and this value is based on the calculation of the infinity norm of Eq. (55) and depicted in Fig. 7. It is seen that the maximum value occurs in the $z$ direction, which is about 1.4 m/s$^2$.

Figure 8 shows the results. The tracking errors along each axis are relatively small, compared with Figs. 4 and 5. In Fig. 9, the control force along each axis is displayed, showing the chattering problem that arises when conventional sliding mode control is used, i.e., high-frequency oscillations in the control force. This chattering phenomenon is more clearly observed in Fig. 10 in which the control force $\boldsymbol{u}$ in the $y$ direction is magnified and plotted only for 0.01 second (between 8.40 and 8.41 seconds). One observes that conventional sliding mode control generates a kind of bang-bang control with the maximum value of $u$ of 4.0 m/s$^2$. This shows that the last term, $-\frac{K_i}{m_i}\text{sgn}(s_i)$, in Eq. (30) domi-

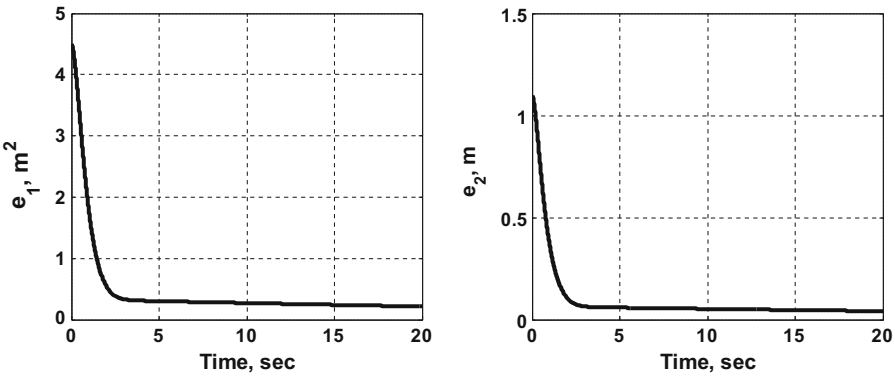


**Fig. 4** Errors of the actual pendulum in the satisfaction of the trajectory requirement given in Eqs. (51a) and (51b) with $\boldsymbol{u} = \mathbf{0}$

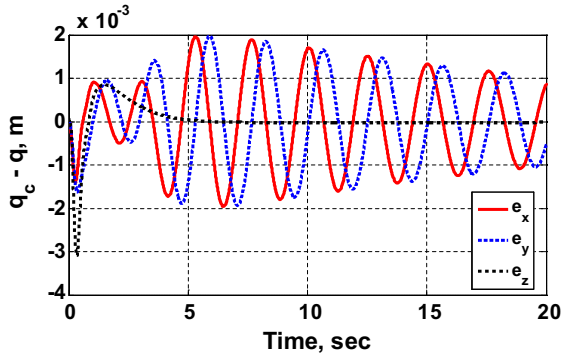


**Fig. 5** Tracking errors ($\boldsymbol{q}_c - \boldsymbol{q}$) between the controlled actual system and the nominal system using the PID controller Eq. (57)

nates the control force $\boldsymbol{u}$, and this term is seen to be very sensitive to the value of $K_i$ [i.e., $\Gamma$, $\mu_m$, and $\mu_M$ (see Eq. 31)] that is chosen for describing the uncertainty $\delta\ddot{\boldsymbol{q}}$ and $\mathbf{M}_a$, respectively.

For comparison, the new PID sliding mode controller given by Eq. (38) that is proposed in this paper is used for the same problem. We use the parameters, $b_i = 10$, $k_i = 5$, $\varepsilon = 0.001$, $\mu_m = 0.1$, $\mu_M = 0.3$, $\Gamma = 2$, and $\eta = 0$. Figure 11 shows the tracking errors between the actual, controlled system and the nominal system along each axis. Comparing with Fig. 8, one observes that the tracking errors are a little larger than those in Fig. 8, but it will be shown shortly that the errors can be further reduced using a larger $\Gamma$. In Fig. 12, the additional control force $u$ along each axis is depicted. The magnitude of the control force is again seen to be much smaller, compared with Fig. 9, and more importantly, the chattering problem is completely removed. Figure 13, which plots the control force $\boldsymbol{u}$ in the $y$ direction for the same time range as in Fig. 10, clearly shows chattering-free continuous control. As illustrated here, the new PID sliding mode control effectively removes chattering and is superior to conventional sliding mode control in reducing the magnitude of the control effort $\boldsymbol{u}$. It is also flexible to be adjusted to yield smaller tracking errors than the conventional PID controller as is shown later on. Figure 14 simultaneously depicts the total control force $\boldsymbol{Q}^c + \boldsymbol{Q}^u$ (dashed lines) and the additional control force $\boldsymbol{Q}^u$ (solid lines) obtained by Eq. (38), which shows a little contribution of $\boldsymbol{Q}^u$ to the total control force.

It should be observed that the control $\boldsymbol{Q}^u$ is a small fraction (10% to 15%) of the total control force $\boldsymbol{Q}^c + \boldsymbol{Q}^u$ though uncertainties in the mass of the bob and the air drag coefficient are both about 20%, in addition to the 9% uncertainty in the value of the gravitational acceleration $g$.

In order to see the effects that the selection of the values for the bounds may have, the same simulation has been performed assuming the same parameters, $b_i = 10$, $k_i = 5$, $\varepsilon = 0.001$, $\mu_m = 0.1$, $\mu_M = 0.3$, and $\eta = 0$, except for $\Gamma = 20$ which is a much more conservative guestimate as might happen in a real-life situation. Figure 15 shows the tracking errors which are about 10 times smaller than those in Figs. 5 and 8 and also smaller than those in Fig. 11, because $\Gamma$ becomes 10 times larger, or equivalently $\varepsilon$ effectively becomes 10 times smaller. However, this larger estimate of the value of $\Gamma$ does not affect the control effort much as reported in [29]. As seen in Fig. 16, the control force $u$ is little changed, compared with Fig. 12 where $\Gamma = 2$ is used. Figure 17 depicts the small differences between the control forces when $\Gamma = 2$ is employed and those when $\Gamma = 20$ is used. During the initial transient phase, relatively large differences are observed because when $\Gamma = 20$, larger control forces are necessary to constrain

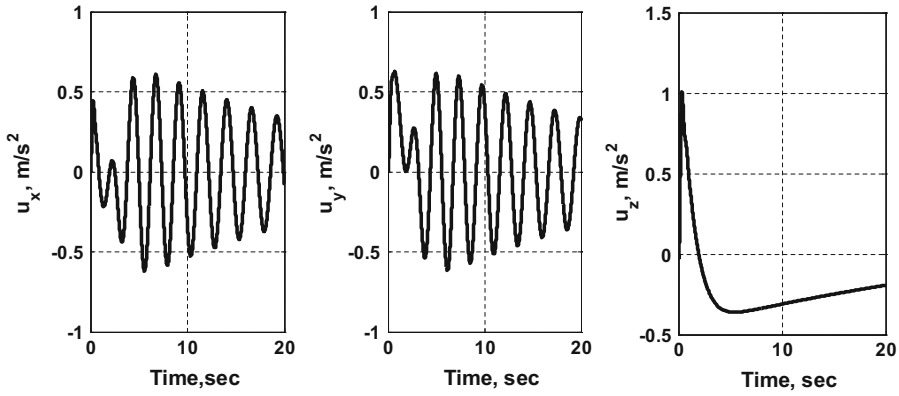


**Fig. 6** Additional control force $\boldsymbol{u}$ along each axis with the PID controller Eq. (57)

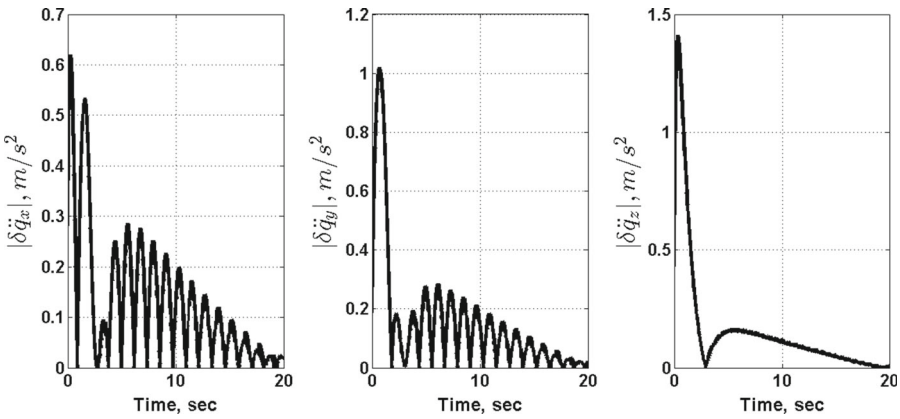


**Fig. 7** Infinity norm of Eq. (55) to calculate $\Gamma$

$|s_i|$ into a smaller region. More specifically, a measure of the overall control cost as measured by $\Delta E$ defined by

$$\Delta E_i = \int_0^{t_f} |u_i|\, dt, \ (i = x, y, z) \tag{58}$$

for both cases is shown in Table 1. Clearly, the required control costs are quite insensitive to the variation of the uncertainty bound $\Gamma$. The reason for this insensitivity will be resolved in future work.

Next, let us see the effects of the bounds for mass uncertainty. The same simulation has been executed assuming the parameters, $b_i = 10$, $k_i = 5$, $\varepsilon = 0.001$, $\Gamma = 2$, and $\eta = 0$, but with $\mu_m = 0.01$ and $\mu_M = 3$, which is a very poor estimate for the mass uncertainty. The tracking errors and the additional control force $\boldsymbol{u}$ are shown in Figs. 18 and 19, respectively. The errors are again about 10 times smaller than those in Fig. 11. It is seen that the smaller estimate of $\mu_m$ and the larger estimate of $\mu_M$ used here do not change the control effort much, as seen in Fig. 19 and as compared with Fig. 12. Figure 20 presents the small differences between the control forces when $\mu_m = 0.01$ and

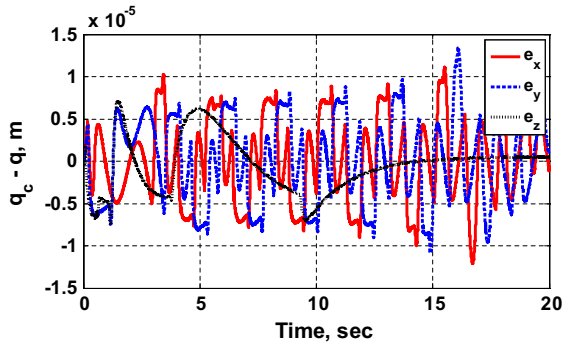


**Fig. 8** Tracking errors ($\boldsymbol{q}_c - \boldsymbol{q}$) between the controlled actual system and the nominal system using the conventional sliding mode controller Eq. (30)

$\mu_M = 3$ is employed and those when $\mu_m = 0.1$ and $\mu_M = 0.3$ is used. As in the larger $\Gamma$ case, in Fig. 20 relatively large differences are observed during the initial transient phase; however, the total control costs again appear to be insensitive to the choices of $\mu_m$ and $\mu_M$, as indicated in Table 1.

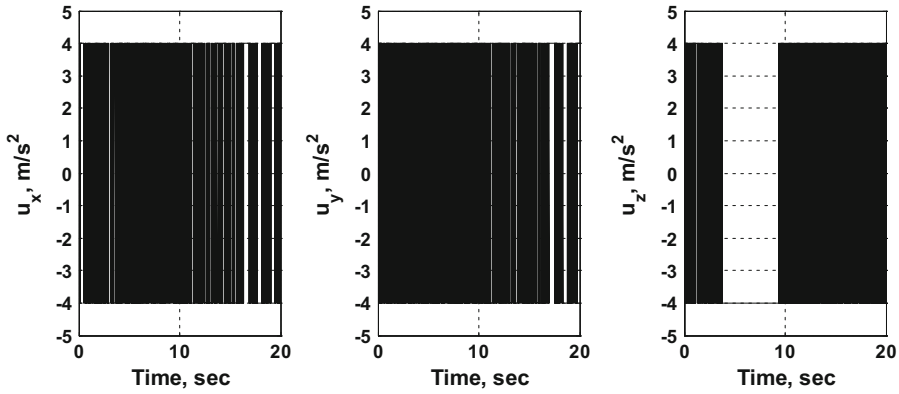


**Fig. 9** Additional control force $\boldsymbol{u}$ along each axis with conventional sliding mode controller Eq. (30)

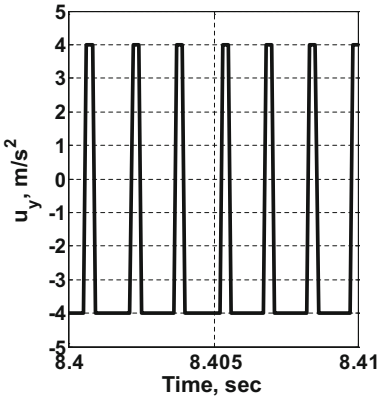


**Fig. 10** Chattering phenomenon generated with conventional sliding mode controller Eq. (30)

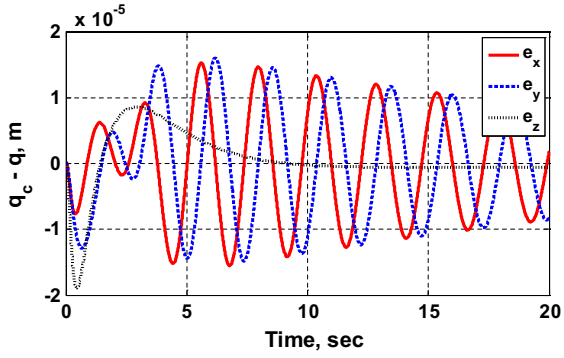


**Fig. 11** Tracking errors ($\boldsymbol{q}_c - \boldsymbol{q}$) between the controlled actual system and the nominal system using the new PID sliding mode controller Eq. (38)

## 4.2 Triple pendulum

To demonstrate the applicability of the proposed methodology for the second controller (for the nondiagonal mass matrix case), a simple multi-body system consisting of a triple pendulum is considered.

The planar pendulum consists of three masses $m_1$, $m_2$, and $m_3$ suspended from massless rods of lengths $L_1$, $L_2$, and $L_3$ moving in the XY-plane (see Fig. 21). An inertial frame of reference is fixed at the point of suspension, $O$, and the potential energy is measured using the line OX as the datum. Though simple, the system can exhibit complex dynamics.

The masses are constrained to move so that the total energy, $E(t)$, of the system is required to equal the sum of the energies (kinetic and potential) of only the two masses $m_2$ and $m_3$, i.e., $E(t) = E_2(t) + E_3(t)$, where we have denoted $E_i(t)$ as the total energy of mass $m_i$.

Using the generalized coordinate 3-vector $\boldsymbol{q}(t) = [\theta_1(t), \theta_2(t), \theta_3(t)]^{\mathrm{T}}$ whose components, in the absence of the above-mentioned energy constraint, are independent of one another, Lagrange's equation for the system is first written down and yields

$$\mathbf{M}\left(\boldsymbol{q}; m_1, m_2, m_3, g\right) \ddot{\boldsymbol{q}} = \boldsymbol{Q}\left(\boldsymbol{q}, \dot{\boldsymbol{q}}; m_1, m_2, m_3, g\right), \tag{59}$$

where the elements of the 3 by 3 symmetric matrix $\mathbf{M}$ are given by

$$\begin{aligned} M_{11} &= (m_1 + m_2 + m_3)L_1^2; \\ M_{12} &= (m_2 + m_3)L_1 L_2 \cos(\theta_{12}); \\ M_{13} &= m_3 L_1 L_3 \cos(\theta_{13}) \\ M_{22} &= (m_2 + m_3)L_2^2; \\ M_{23} &= m_3 L_2 L_3 \cos(\theta_{23}); \;\; M_{33} = m_3 L_3^2, \end{aligned} \tag{60}$$

and the elements of the 3-vector $\boldsymbol{Q}$ are given by (see Eq. (1))

$$\begin{aligned} Q_1 = &-(m_2 + m_3)L_1 L_2 \dot{\theta}_2^2 \sin(\theta_{12}) - m_3 L_1 L_3 \dot{\theta}_3^2 \sin(\theta_{13}) \\ &-(m_1 + m_2 + m_3) g L_1 \sin\theta_1 \end{aligned}$$

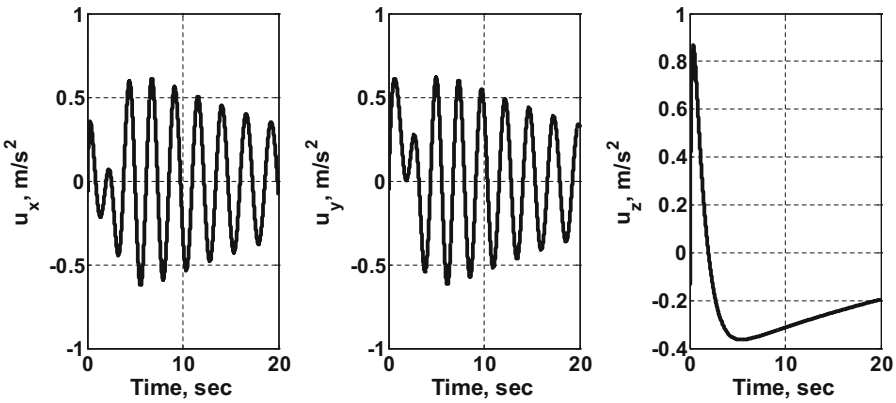


**Fig. 12** Control force $\boldsymbol{u}$ along each axis with the new PID sliding mode controller Eq. (38)

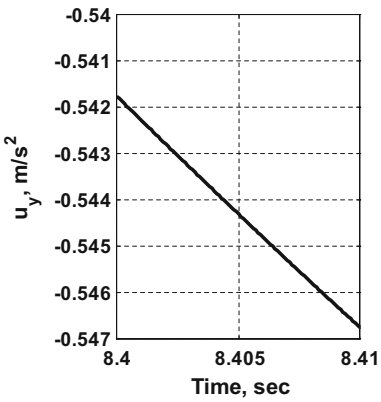


**Fig. 13** Chattering-free continuous control with the new PID sliding mode controller Eq. (38)

$$
\begin{aligned}
Q_2 &= (m_2+m_3)L_1L_2\dot{\theta}_1^2\sin(\theta_{12}) \\
&\quad - m_3L_2L_3\dot{\theta}_3^2\sin(\theta_{23}) - (m_2+m_3)gL_2\sin\theta_2 \\
Q_3 &= m_3L_1L_3\dot{\theta}_1^2\sin(\theta_{13}) \\
&\quad + m_3L_2L_3\dot{\theta}_2^2\sin(\theta_{23}) - m_3gL_3\sin\theta_3. \qquad (61)
\end{aligned}
$$

In the above, we have denoted $\theta_{ij}(t) = \theta_i(t) - \theta_j(t)$, and we explicitly show in Eq. (59) the physical parameters $m_1$, $m_2$, and $m_3$, and the gravitational acceleration parameter $g$, which we will later on consider to be known only imprecisely. As seen in Eq. (60), the elements of the mass matrix $\mathbf{M}$ are now functions of the 3-vector $\boldsymbol{q}$.

In the second step, we describe the energy constraint $E(t) = E_2(t) + E_3(t)$, which is equivalent to the relation $E_1(t) = 0$, where the energy $E_1$ of mass $m_1$ is given by

$$
E_1 = \frac{1}{2}m_1L_1^2\dot{\theta}_1^2 - m_1gL_1\cos\theta_1. \qquad (62)
$$

Since the system may not initially (at time $t = 0$) satisfy the nonholonomic constraint $E_1(t) = 0$, we modify the constraint using the trajectory stabilization relation (Eq. 11):

$$
\dot{E}_1 + \alpha E_1 = 0, \qquad (63)
$$

where $\alpha > 0$ is a positive function. By Eq. (62) and Eq. (63), we obtain the constraint equation

$$
\begin{aligned}
\mathbf{A}\ddot{\boldsymbol{q}} &:= \left[\, L_1^2\dot{\theta}_1 \;0\;0 \,\right]\ddot{\boldsymbol{q}} = -gL_1\sin\theta_1\dot{\theta}_1 \\
&\quad -\alpha\left(\frac{1}{2}L_1^2\dot{\theta}_1^2 - gL_1\cos\theta_1\right) =: \boldsymbol{b}. \qquad (64)
\end{aligned}
$$

To obtain the equations of motion of the (constrained/controlled) nominal system, in the final step we use the information from Eqs. (59)-(61) and Eq. (64) in Eq. (7), and get

$$
\ddot{\boldsymbol{q}} = \boldsymbol{a} + \mathbf{M}^{-1}\mathbf{A}^{\mathrm{T}}(\mathbf{A}\mathbf{M}^{-1}\mathbf{A}^{\mathrm{T}})^{+}(\boldsymbol{b} - \mathbf{A}\boldsymbol{a}). \qquad (65)
$$

In what follows, we shall assume that the real-life triple pendulum described above has masses whose values are imprecisely known and that our best assessment of their (nominal) values is: $m_1 = 1$ (kg), $m_2 = 2$ (kg), and $m_3 = 3$ (kg). The lengths of the massless rods are $L_1 = 1$ (m), $L_2 = 1.5$ (m), and $L_3 = 2$ (m). At $t = 0$, the masses are located with the angles of $\theta_1(0) = 1$ (rad), $\theta_2(0) = 0$ (rad), and $\theta_3(0) = 0$ (rad) (see Fig. 21). The initial velocities are taken to be $\dot{\theta}_1(0) = 0.01$ (rad/s), $\dot{\theta}_2(0) = 0$ (rad/s), and $\dot{\theta}_3(0) = 0$ (rad/s). Since these initial conditions do not satisfy the constraint, $E_1 = 0$, the parameter $\alpha$ in Eq. (63) is chosen to be $0.1\,\|\mathbf{A}\|_2^2$ where $\|\mathbf{A}\|_2$ is the $L^2$ norm of the matrix $\mathbf{A}$ in Eq. (64). The acceleration due to gravity is downwards, and its nominal value is taken to be $g = 9.81$ (m/s$^2$). Numerical integration throughout this example is done in the MATLAB environment,

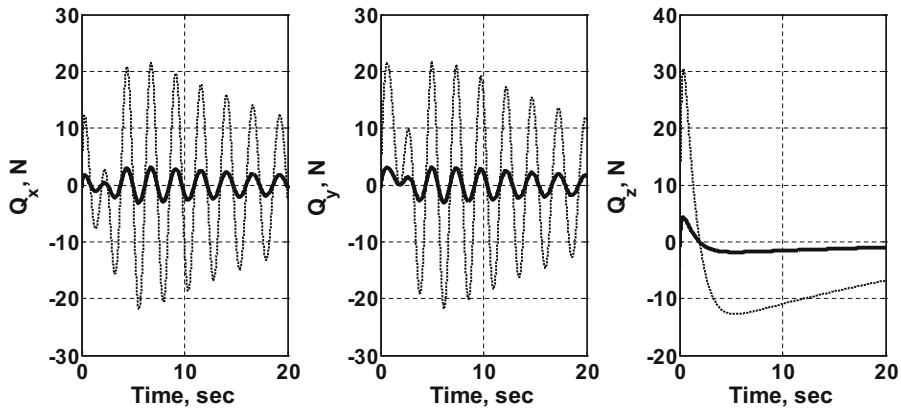


**Fig. 14** Total control force $\boldsymbol{Q}^c + \boldsymbol{Q}^u$ (dashed) and the additional control force $\boldsymbol{Q}^u$ (solid)

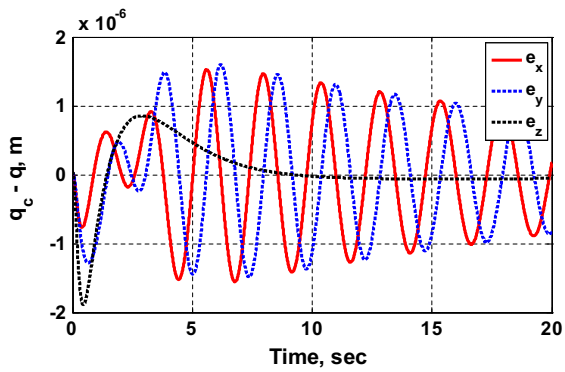


**Fig. 15** Tracking errors ($\boldsymbol{q}_c - \boldsymbol{q}$) between the controlled actual system and the nominal system using the new PID sliding mode controller Eq. (38) when $\Gamma = 20$

using a variable time step integrator with a relative error tolerance of $10^{-8}$ and an absolute error tolerance of $10^{-12}$.

Figure 22 plots the trajectory of mass $m_3$ of the triple pendulum in the XY-plane for a period of 10 seconds. The start of the trajectory is marked by a circle, and its end is marked by a square. The energy of mass $m_1$ versus time $t$ is shown in Fig. 23a. Figure 23b shows the control force $\boldsymbol{Q}^c$ so that the nominal system follows the desired constraint $E_1 = 0$. No control torques are applied to $m_2$ and $m_3$. Figure 23c shows the $L^2$ norm of $\boldsymbol{Q}^c$.

We next consider the actual system and suppose that there is an uncertainty of up to $\pm 10\%$ in each of the nominal values that were used for the three masses $m_1$, $m_2$, and $m_3$. We also assume that the acceleration, $g$, due to gravity is uncertain with a maximum amplitude of $\pm 5\%$ of its nominal value of 9.81 m/s$^2$. Thus both the parameters describing the system and the gravitational force acting on it are uncertain.

With imperfect knowledge of the three masses as well as the magnitude of the force of gravity that acts on the actual system, the actual system's motion is controlled so that it tracks the motion of the controlled (constrained) nominal system and thereby satisfies the constraints imposed on the nominal system. The controller $\boldsymbol{u}$ given by Eq. (47) is used.

The equation of motion of the controlled actual system, Eq. (16), then becomes

$$\ddot{\boldsymbol{q}}_c = a_a + \mathbf{M}_a^{-1}\boldsymbol{Q}^c(t) - \mathbf{M}_a^{-1}\left[\left(\frac{\lambda_M \Gamma}{\varepsilon} + \lambda_M \frac{\|\mathbf{B}\dot{\boldsymbol{e}} + \mathbf{K}\boldsymbol{e}\|_\infty}{\varepsilon} + \eta\right)\left(\dot{\boldsymbol{e}} + \mathbf{B}\boldsymbol{e} + \mathbf{K}\int \boldsymbol{e}dt\right)\right]. \quad (66)$$

The aim is to have the actual system track the trajectory of the nominal system *as though no uncertainty exists in the prescription of the parameters of the nominal system*. As explained in Sect. 3, this is done using the additional controller $\boldsymbol{u}$ that compensates for the uncertainties in our knowledge of the actual system.

In order to illustrate the efficacy of our control method in compensating for our lack of exact knowledge of the actual system, we pick the set $\delta m_1 = 0.1$ (kg), $\delta m_2 = -0.2$ (kg), $\delta m_3 = 0.3$ (kg), and $\delta g = 0.49$ (m/s$^2$) which are assumed to represent our actual system. To check the performance of our controller, we perform a simulation using Eq. (66) by choosing $\Gamma = 40$, and the parameters $k = 10$, $b = k$, $\eta = 50$, $\varepsilon = 10^{-2}$, and $\lambda_M = 30$ to specify our controller. It should be noted that the chosen set of parameters of the actual system, namely $m_1 + \delta m_1 = 1.1\ (kg)$, $m_2 + \delta m_2 = 1.8\ (kg)$, $m_3 + \delta m_3 = 3.3\ (kg)$,

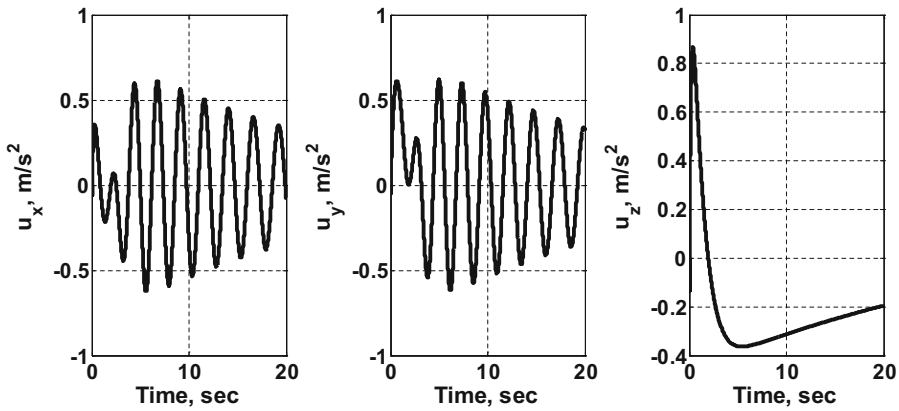


**Fig. 16** Control force $\boldsymbol{u}$ along each axis with the new PID sliding mode controller Eq. (38) when $\Gamma = 20$

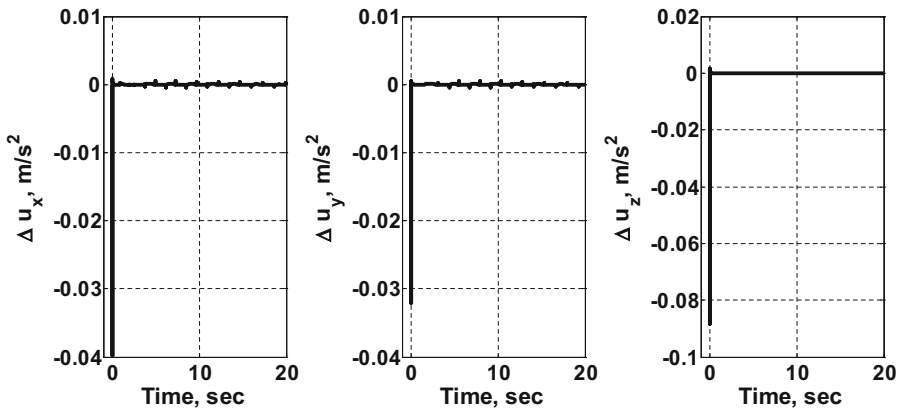


**Fig. 17** Differences between the control forces $\boldsymbol{u}$ when $\Gamma = 2$ and those when $\Gamma = 20$

and $g+\delta g = 10.3$ (m/s$^2$), represents simply one possibility for the parameter set of the actual system, which we use here solely for purposes of demonstration. Also, the values of $\Gamma$ and $\lambda_M$ are simply guestimates of the error bounds, and in practice they could be appropriately chosen. Usually, they are based on intuition, experimentation, or, as in this case, past experience with such a system [12]. As shown below, precise values for these bounds are not necessary as long as they are sufficiently conservative.

The trajectories of the three masses of the actual system follow near-exactly those of the nominal system (Fig. 22) and have not been shown for brevity. The maximum (generalized) displacement error $\boldsymbol{q}_c - \boldsymbol{q}$ and (generalized) velocity error $\dot{\boldsymbol{q}}_c - \dot{\boldsymbol{q}}$ between the nominal system Eq. (65) and the controlled actual system Eq. (66) are computationally found to be of the order of $O(10^{-5})$ and $O(10^{-4})$ as shown in Figs. 24 and 25, respectively.

This illustrates the performance of the closed-form controller proposed in Sect. (3.2); the controlled actual system tracks the trajectories pre-specified by the nominal system in the presence of the $\pm 10\%$ uncertainties in the masses of the system and the $\pm 5\%$ uncertainty in gravity field, along with the constraint imposed on it given by Eq. (63). Also, the continuous control functions in Eq. (47) eliminate chattering.

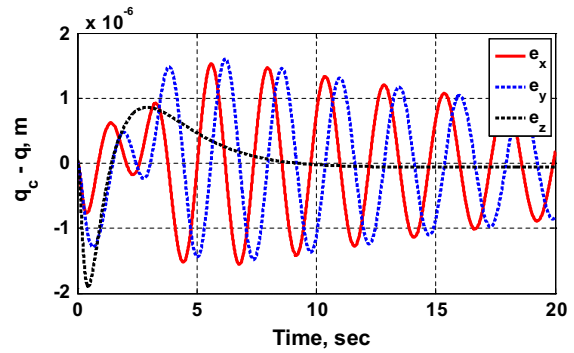


**Fig. 18** Tracking errors ($\boldsymbol{q}_c - \boldsymbol{q}$) between the controlled actual system and the nominal system using the new PID sliding mode controller Eq. (38) when $\mu_m = 0.01$ and $\mu_M = 3$

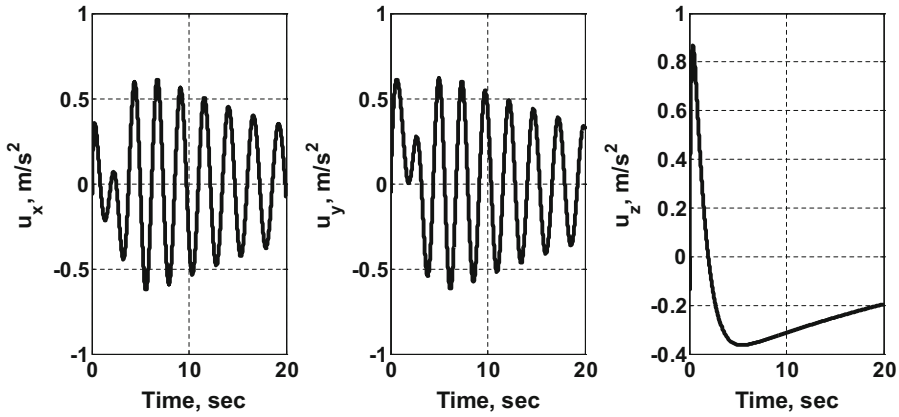


**Fig. 19** Control force $\boldsymbol{u}$ along each axis with new PID sliding mode controller Eq. (38) when $\mu_m = 0.01$ and $\mu_M = 3$

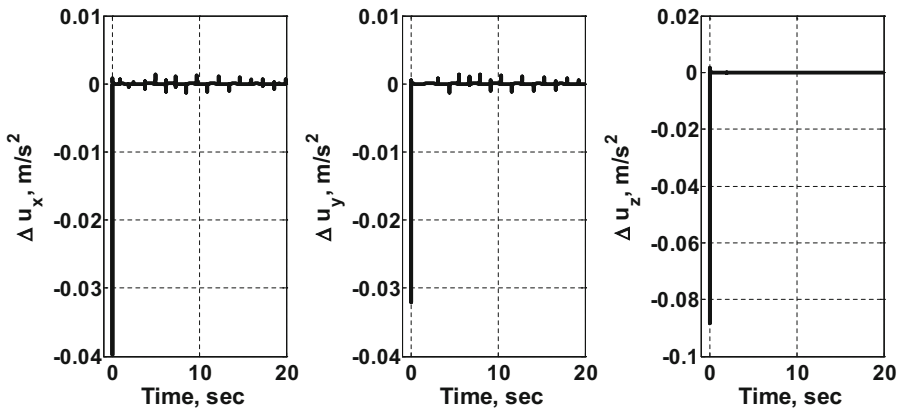


**Fig. 20** Differences between the control forces $\boldsymbol{u}$ when $\mu_m = 0.1,\ \mu_M = 0.3$ and those when $\mu_m = 0.01$ and $\mu_M = 3$

**Table 1** Control costs

| | $\Gamma = 2,\ \mu_m = 0.1,\ \mu_M = 0.3$ | $\Gamma = 20,\ \mu_m = 0.1,\ \mu_M = 0.3$ | $\Gamma = 2,\ \mu_m = 0.01,\ \mu_M = 3$ |
|---|---|---|---|
| $\Delta E_x$ (m/s) | 5.8207 | 5.8211 | 5.8212 |
| $\Delta E_y$ (m/s) | 6.1812 | 6.1818 | 6.1818 |
| $\Delta E_z$ (m/s) | 5.9120 | 5.9125 | 5.9125 |
| $\Delta E_{Total}$ (m/s) | 17.9139 | 17.9154 | 17.9155 |

The total control torques, $\boldsymbol{u}$, applied to the actual pendulum, on the masses $m_1, m_2$, and $m_3$ are shown in Fig. 26. Figure 26d depicts the $L^2$ norm of all control torques from three masses.

Now, we provide another example in which all the parameters are identical to those specified in the previous triple pendulum example except for the values of the uncertainty bounds $\Gamma$ and $\lambda_M$ which, recall, were simply guessed before. We now use much more conservative bounds for these parameters, namely $\Gamma = 400$ and $\lambda_M = 50$.

Of course, the trajectories of the three masses of the actual system also follow near-exactly those of the nominal system (Fig. 22). However, the maximum generalized displacement error $\boldsymbol{e} = \boldsymbol{q}_c - \boldsymbol{q}$ and generalized velocity error $\dot{\boldsymbol{e}} = \dot{\boldsymbol{q}}_c - \dot{\boldsymbol{q}}$, shown in Figs. 27 and 28, respectively, are substantially smaller when compared with the results shown in Figs. 24 and 25.

We note that while the tracking errors reduce, the control effort does not change appreciably (see Fig. 29), as in the example of the spherical pendulum in Section 4.1 [29]. The magnitudes of the control torques that make the actual system mimic the behavior of the nominal system are comparable with the ones shown in Fig. 26. The results in Figs. 24, 25, 26, 27, 28 and 29 show an improvement over those obtained in Refs.

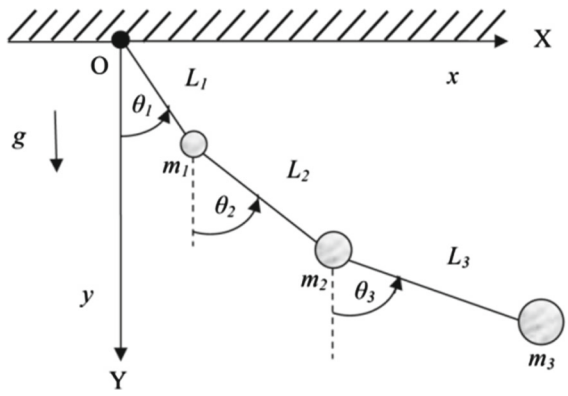


**Fig. 21** Triple pendulum with the datum at origin O

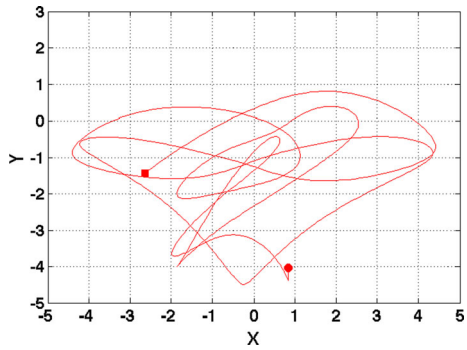


**Fig. 22** Motion of mass $m_3$ (m), starting at the circle

[12] and [32] that use a very different generalized sliding mode control strategy to obtain the additional controller $\boldsymbol{u}$ that compensates for the presence of uncertainties, along with $f_i(s) = \eta s_i^3,\ \eta \geq 0$ (see Eq. (46)). In addition to employing a completely different control strategy, the use of Eq. (46) allows the controller used here to be of the more familiar PID type, which has a long history of usage and can be very easily implemented.

## 5 Conclusions

Two new continuous sliding mode controllers for reference tracking were proposed. Two independent control strategies were developed and combined to precisely track the required reference trajectory even in the face of substantial uncertainties. The first controller was derived for reference control input, employing the concept of the FECM. Development of the second controller constituted the core part of this paper. By tak-

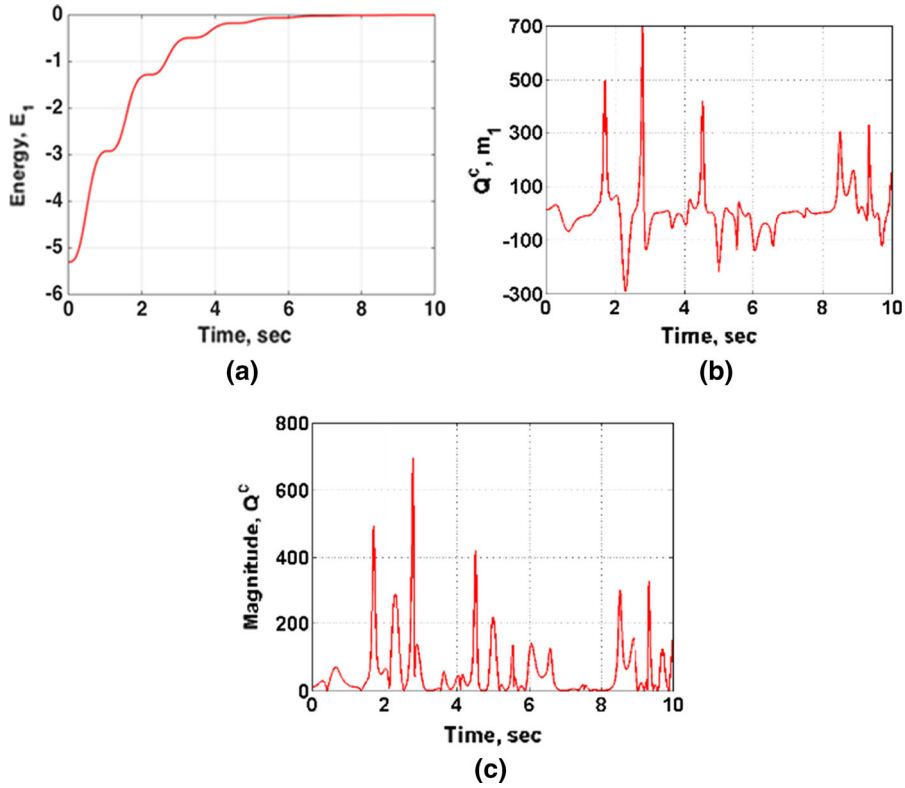


**Fig. 23** **a** Energy $E_1$ in N-m, **b** constraint torque (N-m) on mass $m_1$ of the nominal system to satisfy the constraint $E = E_2 + E_3$ **c** $L^2$ norm of constraint torque

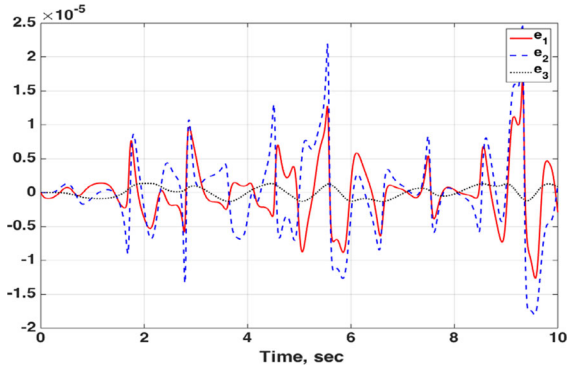


**Fig. 24** Displacement tracking errors (rad) between the controlled nominal system and the controlled actual system $(q_c - q)$

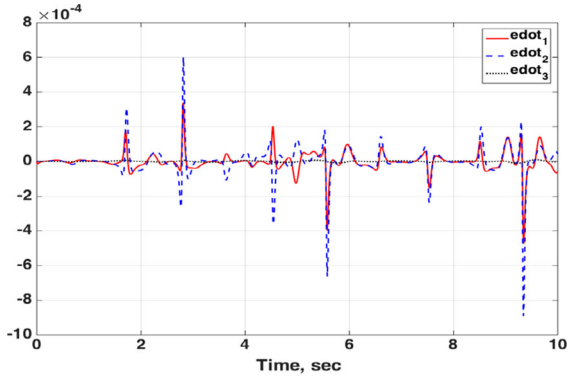


**Fig. 25** Velocity tracking errors (rad/s) between the controlled nominal system and the controlled actual system $(\dot{q}_c - \dot{q})$

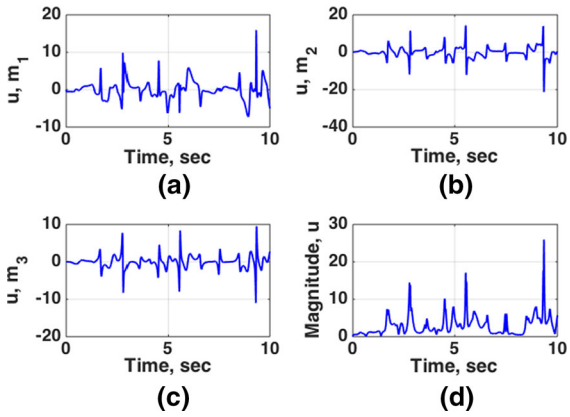


**Fig. 26** Control torques (rad/s$^2$) on the controlled actual system; **a** mass $m_1$, **b** $m_2$, **c** $m_3$, and **d** $L^2$ norm of control torques

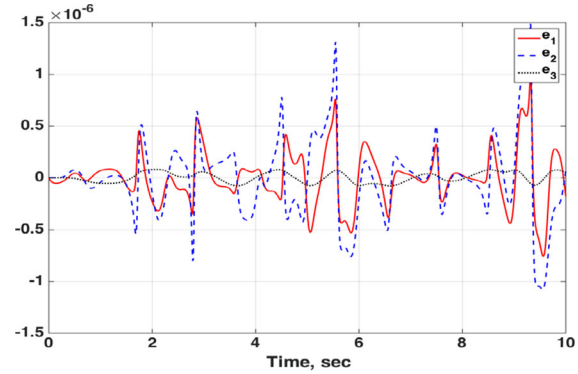


**Fig. 27** Displacement tracking errors (rad) between the controlled nominal system and the controlled actual system $(q_c - q)$ when $\Gamma = 400$ and $\lambda_M = 50$

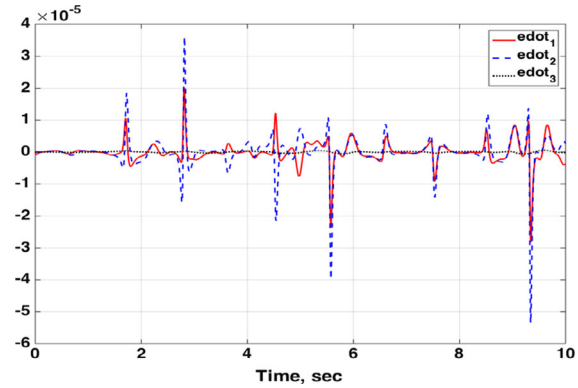


**Fig. 28** Velocity tracking errors (rad/s) between the controlled nominal system and the controlled actual system $(\dot{q}_c - \dot{q})$ when $\Gamma = 400$ and $\lambda_M = 50$

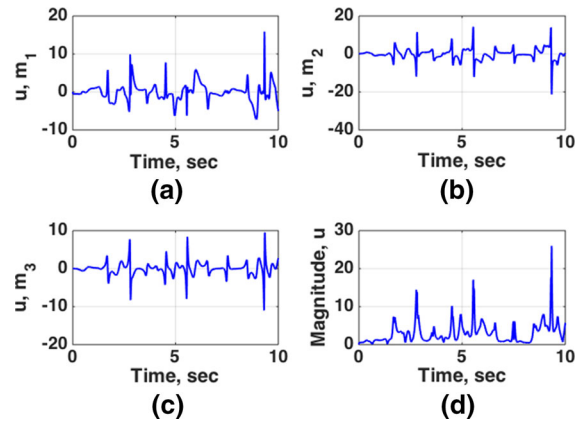


**Fig. 29** Control torques (rad/s$^2$) on the controlled actual system; **a** mass $m_1$, **b** $m_2$, **c** $m_3$, and **d** $L^2$ norm of control torques when $\Gamma = 400$ and $\lambda_M = 50$

ing into account uncertainties in the masses and in the given forces, new sliding mode controllers were designed that use continuous functions to remove chattering according to whether the mass matrix is diagonal or not. Numerous forms of the control function are possible depending on practical considerations, and a simple special PID-form of SMC was shown to provide high robustness. Though the control laws do not force the system trajectories exactly to the sliding surface so the errors do not exactly converge to zero, it is always possible to have these errors as arbitrarily small as desired. Two examples were simulated to demonstrate the efficacy of the new controllers whose use depends on whether the mass matrix is diagonal or non-diagonal.

The control schemes were shown to be robust and insensitive to *guestimates of the uncertainties* in (i) the parameters that describe the dynamical system and (ii) the forces acting on it. This makes these schemes attractive for practical control of real-life complex physical systems in which the *extent* of uncertainties in describing them by mathematical models can, very often, only be poorly estimated.

Future work includes extension of the proposed approach to nonlinear MIMO systems with mismatched uncertainties. Also, an adaptive method will be developed such that control parameters are automatically tuned and one need not measure or estimate the bounds on the uncertainties.

**Compliance with ethical standards**

**Conflicts of interest** The authors declare that they have no conflict of interest.

**Human and animal rights** The research carried out in this article did not involve any human participants or animals.

**Informed consent** Consent to submit has been received explicitly from all co-authors. The research did not involve any human participants.

## Appendix

In this "Appendix", Eq. (32) is proven when $|s_i| > \varepsilon$ holds. If $s_i$ and $\delta\ddot{\boldsymbol{q}}_i$ have opposite signs, then Eq. (32) always holds because the right-hand side is always positive. Hence, let us consider the following two cases in which $s_i$ and $\delta\ddot{\boldsymbol{q}}_i$ have the same sign.

**Case 1** When $s_i > 0$ and $0 \le \delta\ddot{\boldsymbol{q}}_i < \Gamma$, since $s_i > 0$, we have

$$\frac{s_i}{\varepsilon} > 1 \tag{A1}$$

from the assumption of $|s_i| > \varepsilon$. Multiplying both sides by $\Gamma s_i$ $(> 0)$ yields

$$\Gamma s_i < \frac{\Gamma}{\varepsilon} s_i^2. \tag{A2}$$

From the assumption that $s_i > 0$ and $\delta\ddot{q}_i < \Gamma$, we have

$$s_i \delta\ddot{q}_i < \Gamma s_i, \tag{A3}$$

and from Eq. (A2) it follows that $s_i \delta\ddot{q}_i < \frac{\Gamma}{\varepsilon} s_i^2$.

**Case 2** When $s_i < 0$ and $-\Gamma < \delta\ddot{q}_i \le 0$, since $s_i < 0$, $|s_i| = -s_i$ and again from $|s_i| > \varepsilon$, we have

$$-\frac{s_i}{\varepsilon} > 1. \tag{A4}$$

Multiplying both sides by $-\Gamma s_i$ $(> 0)$ yields

$$-\Gamma s_i < \frac{\Gamma}{\varepsilon} s_i^2. \tag{A5}$$

From the assumption that $s_i < 0$ and $-\Gamma < \delta\ddot{q}_i$, we have

$$s_i \delta\ddot{q}_i < -\Gamma s_i, \tag{A6}$$

and it follows from Eq. (A5) that $s_i \delta\ddot{q}_i < \frac{\Gamma}{\varepsilon} s_i^2$, and this completes the proof.

## References


1. Åström, K.J., Wittenmark, B.: Computer-Controlled Systems: Theory and Design, 3rd edn. Prentice-Hall, Upper Saddle River (1996)
2. Rawlings, J.B.: Model Predictive Control: Theory and Design. Nob Hill Pub, Portland (2009)
3. Ikhouane, F., Krstic, M.: Robustness of the tuning functions adaptive backstepping design for linear systems. IEEE Trans. Autom. Control **43**, 431–437 (1998)
4. Utkin, V.: Sliding Modes in Control and Optimization. Springer, Berlin (1992)
5. Edwards, C., Spurgeon, S.: Sliding Mode Control: Theory and Applications. Taylor & Francis, Boca Raton (1998)
6. Slotine, J.J., Sastry, S.S.: Tracking control of nonlinear systems using sliding surfaces with application to robot manipulator. Int. J. Control **38**, 465–492 (1983)
7. Burton, J.A., Zinober, A.S.: Continuous approximation of variable structure control. Int. J. Syst. Sci. **17**, 875–885 (1986)
8. Li, M., Wang, F., Gao, F.: PID-based sliding mode controller for nonlinear processes. Ind. Eng. Chem. Res. **40**, 2660–2667 (2001)

9. Laghrouche, S., Plestan, F., Glumineau, A.: Higher order sliding mode control based on integral sliding surface. Automatica **43**, 531–537 (2007)
10. Estrada, A., Fridman, L.M.: Integral HOSM semiglobal controller for finite-time exact compensation of unmatched perturbations. IEEE Trans. Autom. Control **55**, 2645–2649 (2010)
11. Levant, A.: Sliding order and sliding accuracy in sliding mode control. Int. J. Control **58**, 1247–1263 (1993)
12. Udwadia, F.E., Wanichanon, T.: Control of uncertain nonlinear multibody mechanical systems. J. Appl. Mech. **81**, 041020-1–041020-11 (2013)
13. Udwadia, F.E., Wanichanon, T., Cho, H.: Methodology for satellite formation-keeping in the presence of system uncertainties. J. Guidance Control Dyn. **37**, 1611–1624 (2014)
14. Cho, H., Wanichanon, T., Udwadia, F.E.: New continuous control methodology for nonlinear dynamical systems with uncertain parameters. In: Proceedings of the 1st ECCOMAS Thematic Conference on International Conference on Uncertainty Quantification in Computational Sciences and Engineering, Crete, Greece (2015)
15. Wanichanon, T., Cho, H., Udwadia, F.E.: An effective approach for the control of uncertain systems. In: Proceedings of the 23rd ABCM International Congress of Mechanical Engineering, Rio de Janeiro, Brazil (2015)
16. Kalaba, R.E., Udwadia, F.E.: Equations of motion for nonholonomic constrained dynamic systems using Gauss's principle. J. Appl. Mech. **60**, 662–668 (1993)
17. Udwadia, F.E.: Equations of motion for mechanical systems: a unified approach. Int. J. Non-Linear Mech. **31**, 951–958 (1996)
18. Udwadia, F.E.: A new perspective on the tracking control of nonlinear structural and mechanical systems. Proc. R. Soc. Lond. Ser. A **459**, 1783–1800 (2003)
19. Udwadia, F.E.: Optimal tracking control of nonlinear dynamical systems. Proc. R. Soc. Lond. Ser. A **464**, 2341–2363 (2008)
20. Wanichanon, T., Cho, H., Udwadia, F.E.: An approach to the dynamics and control of uncertain multi-body system. Procedia IUTAM **13**, 43–52 (2015)
21. Yang, J., Li, S., Yu, X.: Sliding-mode control for systems with mismatched uncertainties via a disturbance observer. IEEE Trans. Ind. Electron. **60**, 160–169 (2013)
22. Yang, J., Li, S., Su, J., Yu, X.: Continuous nonsingular terminal sliding mode control for systems with mismatched disturbances. Automatica **49**, 2287–2291 (2013)
23. Yang, J., Su, J., Li, S., Yu, X.: High-order mismatched disturbance compensation for motion control systems via a continuous dynamic sliding-mode approach. IEEE Trans. Ind. Inform. **10**, 604–614 (2014)
24. Udwadia, F.E., Kalaba, R.E.: Analytical Dynamics: A New Approach, 1st edn. Cambridge University Press, Cambridge (2007)
25. Udwadia, F.E., Kalaba, R.E.: A new perspective on constrained motion. Proc. R. Soc. Lond. **439**, 407–409 (1992)
26. Udwadia, F.E., Kalaba, R.E.: New directions in the control of nonlinear mechanical systems. In: Guttalu, R.S. (ed.) Mechanics and Control, pp. 81–84. Plenum Press, New York (1994)
27. Skogestad, S., Postlethwaite, I.: Multivariable Feedback Control: Analysis and Design, 2nd edn. Wiley, Hoboken (2005)
28. Kachroo, P.: Existence of solutions to a class of nonlinear convergent chattering-free sliding mode control systems. IEEE Trans. Autom. Control **44**, 1620–1624 (1999)
29. Udwadia, F.E., Koganti, P.B.: Dynamics and control of a multi-body planar pendulum. Nonlinear Dyn. **81**, 845–866 (2015)
30. Dembo, A.: Bounds on the extreme eigenvalues of positive-definite Toeplitz matrices. IEEE Trans. Inf. Theory **34**, 352–355 (1988)
31. Zhan, X.: Extremal eigenvalues of real symmetric matrices with entries in an interval. SIAM J. Matrix Anal. Appl. **27**, 851–860 (2006)
32. Udwadia, F.E., Koganti, P.B., Wanichanon, T., Stipanovic, D.M.: Decentralised control of nonlinear dynamical systems. Int. J. Control **87**, 827–843 (2014)